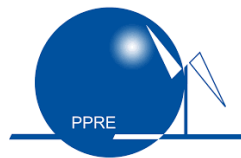




**Carl von Ossietzky Universität Oldenburg**

**Institute of Physics**

**Postgraduate Programme Renewable Energy**



**Master's Thesis**

Title:

**Comparison of dynamic and steady state models for the space  
discrete simulation of heat networks**

**Accuracy and validation under different flow regimes and temperature levels**

Presented by: *Indry Sanyaxel SANCHEZ JOYA*

First examiner: *Prof. Dr. Carsten AGERT*

Second examiner: *Dr. Herena TORIO*

Ext. supervision: *M.sc. Diana MALDONADO*

Place, Date: *Oldenburg, April 27, 2023*



# *Acknowledgements*

I would like to express my gratitude and appreciation to several people and organisations that have played an important role in the realisation of my Master's thesis.

First of all, I would like to thank the University of Oldenburg for giving me the opportunity to pursue a Master's degree. Thanks to the staff members of the PPRE, especially Hans Holtorf, Andreas Guenther and Edu Knagge, who have contributed greatly to my personal and academic growth.

I would also like to thank the Institute of the German Aerospace Center DLR, because I have learned a lot and my knowledge and handling of tools have improved more than I expected in such a short time. Thanks to the EST department for providing me with the necessary support and guidance.

My deepest thanks to my supervisor Dr. Herena Torio, a woman passionate about research and academia, thank you for the guidance and infinite patience with my work at DLR and at the University. Thank you for being my female inspiration in the field of science and in the life. A special thanks to Diana Maldonado, who was always there to help and guide me, thank you for always being open to listen and help in any way you can.

I am also indebted to my family for their unconditional love, encouragement and support. Your faith in me has been a source of motivation and inspiration, even when distance and time difference are big obstacles, you are always there in the good and bad moments.

Finally, I would like to acknowledge and thank all the special people I have met here in Germany, fellow PPRE students, co-workers, and close friends who have been supporting me while teaching me about life, about the world.

Thank you all for helping me to make this dream come true.

# Contents

<b>1</b>	<b>Introduction</b>	<b>1</b>
<b>2</b>	<b>Theory</b>	<b>6</b>
2.1	District heating networks modelling . . . . .	6
2.2	Steady state approach, TESPy . . . . .	7
2.3	Dynamic approach, CarnotTB . . . . .	8
2.4	Discretization methods . . . . .	10
<b>3</b>	<b>Methodology</b>	<b>12</b>
3.1	Projects description . . . . .	13
3.1.1	Scenario ENaQ . . . . .	13
3.1.2	Scenario Lampoldhausen . . . . .	15
3.2	Method to discretize the models . . . . .	19
3.3	Simulations . . . . .	25
<b>4</b>	<b>Results and Discussion</b>	<b>28</b>
4.1	Definition of number of nodes . . . . .	28
4.2	Differences in the results for ENaQ and Lampoldshasen . . . . .	30
4.3	Influence of input parameters . . . . .	35
4.3.1	Soil temperature . . . . .	35
4.3.2	Mass flow . . . . .	37
4.3.3	Inlet temperature . . . . .	46
<b>5</b>	<b>Conclusions and future work</b>	<b>57</b>
5.1	Conclusions . . . . .	57
5.2	Future work . . . . .	60
<b>6</b>	<b>Appendix</b>	<b>61</b>
	<b>Bibliography</b>	<b>63</b>



# List of Figures

1.1	Annual energy supplies to district heating networks in the Net Zero Scenario, World, 2010-2030, modified from [3] . . . . .	2
1.2	Outlet temperature correlation between a dynamic and steady state approach under low temperature conditions, ENaQ, from [7] . . . . .	3
1.3	Heat losses calculation for the dynamic and steady state approach under low temperature conditions, ENaQ, from [7] . . . . .	4
3.1	Simplification of CarnotTB model from [8], to spatially discretize the pipe, ENaQ . . . . .	15
3.2	Complete aerospace center, and selected branch of heat network to study marked in colors, Lampoldshausen, modified from [29] . . . . .	16
3.3	Selected branch of Lampoldshausen heat network, in CarnotTB simulation . . . . .	17
3.4	Matlab code to register the time taken by the software solving the simulations, for ENaQ and Lampoldshausen . . . . .	20
3.5	CarnotTB pipe block setup, from the main pipe fork P1 to fort P2, Lampoldshausen . . . . .	23
3.6	Box and Whiskers Statistical tool for data visualization, modified from [31] . . . . .	24
3.7	Range of operation of HT profile original from ENaQ, and synthetic profile for LT, comparison . . . . .	26
4.1	Reduction of outlet temperature due to spatial discretization for 1n - 5n, ENaQ . . . . .	31
4.2	Increment of energy losses due to spatial discretization for 1n - 5n, ENaQ . . . . .	31
4.3	Reduction of the outlet temperature for 3 months between measurements data vs TESPpy and measured data vs CarnotTB discretized, Lampoldshausen . . . . .	33
4.4	Delta energy values vs mass flow for 1n-5n, ENaQ, Carnot. . . . .	35

4.5	Reduction of the outlet temperatures for ENaQ with the sinusoidal soil temperature vs ENaQ with a fixed soil temperature of 12 °C . . . . .	36
4.6	Energy losses and outlet temperature differences 1n-5n vs mass flow, ENaQ . . . . .	37
4.7	Weekly profiles for winter in January, and summer in July, in a dynamic analysis vs the mass flow, ENaQ . . . . .	38
4.8	RMSE for heat losses and outlet temperature differences between single and multi nodes, for a clustered inlet temperature, ENaQ . . . . .	40
4.9	Reductions in the outlet temperature from the comparison between real data, TESP <sub>y</sub> and CarnotTB vs mass flow, Lampoldshausen . . . . .	41
4.10	Outlet temperature from the the measured data, from the steady state model represented by TESP <sub>y</sub> and from the dynamic model represented by CarnotTB, all compared with the mass flow, Lampoldshausen . . . . .	43
4.11	Correlation between steady state and dynamic models, clustered in 3 equitable ranges of mass flow, Lampoldshausen . . . . .	44
4.12	Outlet temperature behavior for two different mass flows A, differences in the outlet temperature for two different mass flows B. . . . .	45
4.13	Differences in the energy losses and outlet temperature between 1n and 5n vs initial temperature, ENaQ . . . . .	47
4.14	RMSE of the differences in output variables for HT and LT profile, ENaQ	48
4.15	Reductions in the outlet temperature from the comparison between real data, TESP <sub>y</sub> and CarnotTB vs inlet temperature, Lampoldshausen . . . . .	49
4.16	Outlet temperature from the real data, TESP <sub>y</sub> and CarnotTB vs inlet temperature, Lampoldshausen . . . . .	50
4.17	Outlet temperature from the real data, TESP <sub>y</sub> and CarnotTB vs inlet temperature, Lampoldshausen . . . . .	51
4.18	Clustered inlet temperature to get the RMSE of the differences in outlet temperatures, Lampoldshausen . . . . .	52
4.19	Box and whiskers chart for outlet temperatures for the different spatially discretized models, Lampoldshausen . . . . .	53
4.20	Energy losses from 1n-3n and 1n-10n comparison, ENaQ, TESP <sub>y</sub> . . . . .	54
4.21	Initialization behaviour for outlet temperatures for 1n vs 3n and 10n, ENaQ, TESP <sub>y</sub> . . . . .	55
6.1	Description of the scenario 1, discretization visualization and hypothesis	61
6.2	Description of the scenario 2, discretization visualization and hypothesis	62

6.3 Correlation for energy losses and losses temperature for scenario 1,  
between 1n and discreted models 5n, 10n 20n . . . . . 62

## List of Tables

3.1	Description of the two scenarios analyzed, defining for each one the approach, software and proposed simulations comparing the models . .	12
3.2	Summary of input data and parameters for ENaQ and Lampoldshausen	18
4.1	RMSE, length and duration of the software running for 1 year each simulation, in function of the number of nodes, ENaQ . . . . .	29
4.2	Definition of the optimal number of nodes based on ENaQ, for Lampoldshausen . . . . .	30
4.3	Soil temperature range of operation for ENaQ and Lampoldshausen . .	35
4.4	Mass flow range of operation for ENaQ and Lampoldshausen . . . . .	38
4.5	Inlet temperature range of operation for ENaQ and Lampoldshausen . .	46

# Glossary

**ENaQ:** Energetic Neighbourhood Quarter project or *Energetisches Nachbarschaftsquartier Fliegerhorst Oldenburg*.

**RE:** Renewable Energy.

**DH:** District heating.

**DHN:** District heating networks.

**HT:** Hot temperature.

**HTDH:** Hot temperature district heating.

**LT:** Low temperature.

**LTDH:** Low temperature district heating.

**RE:** Renewable energy.

**GHG:** Greenhouse gas.

**RMSE:** Root Mean Square Error.

**TESPy:** Thermal Engineering Systems in Python.

**CarnotTB:** Conventional And Renewable eNergy systems OpTimization Blockset.

**PDE:** partial differential equation(s).

**FD:** Finite difference method.

**Mathematical notation:** "." and "," Thousand notation is done with "dot" i.e. 9.000 kg/h, while decimal notation is with "comma" i.e. 0,28 °C.

x

*Dedicado con amor a mi madre, mi padre, mi hermana y mi  
hermano*

## Chapter 1

# Introduction

In order to prevent worst climate damages caused by the pollution from human activities, the *International Scientific Consensus Net Zero* [1] asks to globally reduce the carbon dioxide emissions to net zero around 2050, one of the main factors contributing to the changing climate is the energy consumption with a considerable effect in the previous decades [2].

Accounting for 50 % of global final energy consumption in 2018, heat is the largest energy end-use contributing with 40 % of global carbon dioxide CO<sub>2</sub> emissions [3], district heating (DH) heat sources come mainly from fossil fuels, as presented in figure 1.1.

The most important reason to focus on the District Heating Networks (DHN) is because approximately 90 % of the worldwide DHN supplies are still strongly dominated by fossil fuels [3], which partially explains the high quantity of CO<sub>2</sub> emissions coming from this activity, but from a sustainable perspective, DHN offer great potential for efficient, cost-effective and flexible large scale integration of low-carbon and renewable energy sources into the heating energy mix [4].

To achieve the Net Zero goal by 2050, is necessary to rapidly switch them to renewable heat sources and improve the energy efficiency of the existing networks, this imply significant efforts in several fields [3] like the simplified models that accurately capture the complex and dynamic thermal phenomena, enabling to evaluate the heat network behavior with a reasonable accuracy [5].

Like the development of simplified models for the complex and dynamic thermal phenomena with reasonable accuracy level for the heat network performance.

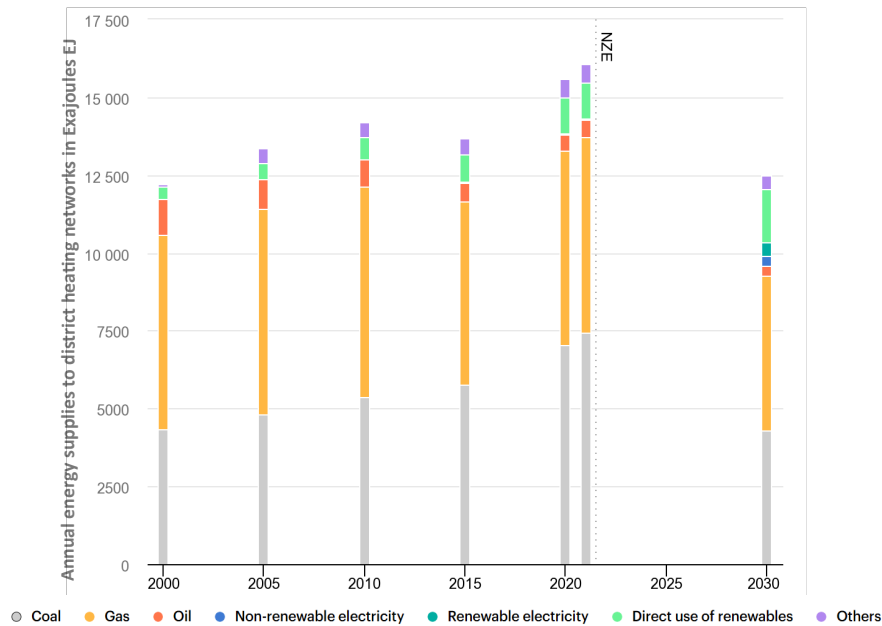


FIGURE 1.1: Annual energy supplies to district heating networks in the Net Zero Scenario, World, 2010-2030, modified from [3]

District heating thermal behaviour can be modelled with simulation approaches based on simplified models like the *steady state*, that can use open source software, are time series based and easy to build and understand, or with *dynamic* models based on existing components in modelling environments such as Modelica, TRNSYS or Matlab, these software consider the entire structure of a DHN, which makes them easy to modify but complex and computationally intensive [5]. In addition to the use of highly complex and dynamic models, simplified approaches such as steady state models aim to engage a balance between model accuracy and simulations size [5], [6].

Results from a recent master thesis Maldonado [7], devoted to investigate the suitability of simplified approaches for modelling the dynamic behaviour of heat networks under different operation temperatures have shown that:

- Steady state approaches show small deviations as compared to fully dynamic models under high flow conditions, i.e. if the mass flow within the network is high.
- The steady state model better matches the accuracy of the dynamic model when both operates under low temperature conditions, the calculations for the outlet temperature has an almost perfect correlation comparing both models, as presented in figure 1.3.



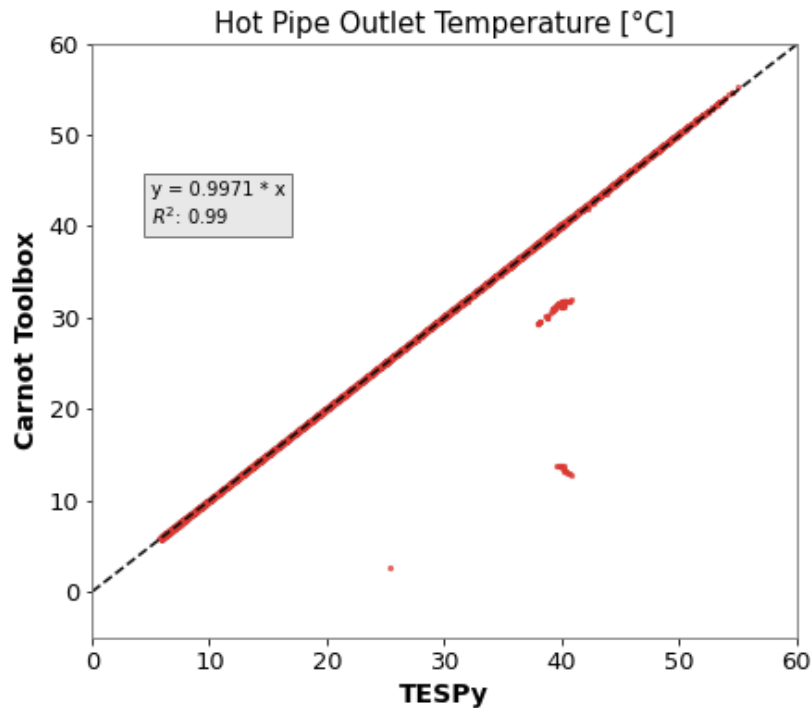


FIGURE 1.2: Outlet temperature correlation between a dynamic and steady state approach under low temperature conditions, ENaQ, from [7]

Nevertheless, there is a clear offset in the heat losses because the steady state model overestimates them, as is presented in figure 1.3.

Here is where the present master thesis aims to contribute investigating the reasons leading to these behaviours. For this, first a thorough analysis of the steady state and dynamic models is required.

Dynamic models implemented in the simulation environment of Carnot Toolbox (Matlab) allow depicting several physical phenomena influencing the heat losses and thermal behaviour of the network. In turn, steady state models (TESPy) overlook thermal inertia and axial heat transfer within the pipe fluid. Considering those thermal phenomena justifies at least partly the differences obtained in the behaviour of dynamic models for heat networks when compared to steady state approaches.

However, in the models used in the aforementioned master thesis [7], that level of detail was not fully deployed and all pipes were modelled as single nodes considering the thermal inertia, but excluding the axial heat transfer phenomena [8]. the mentioned work utilizes for the simulation one spatial step size which is

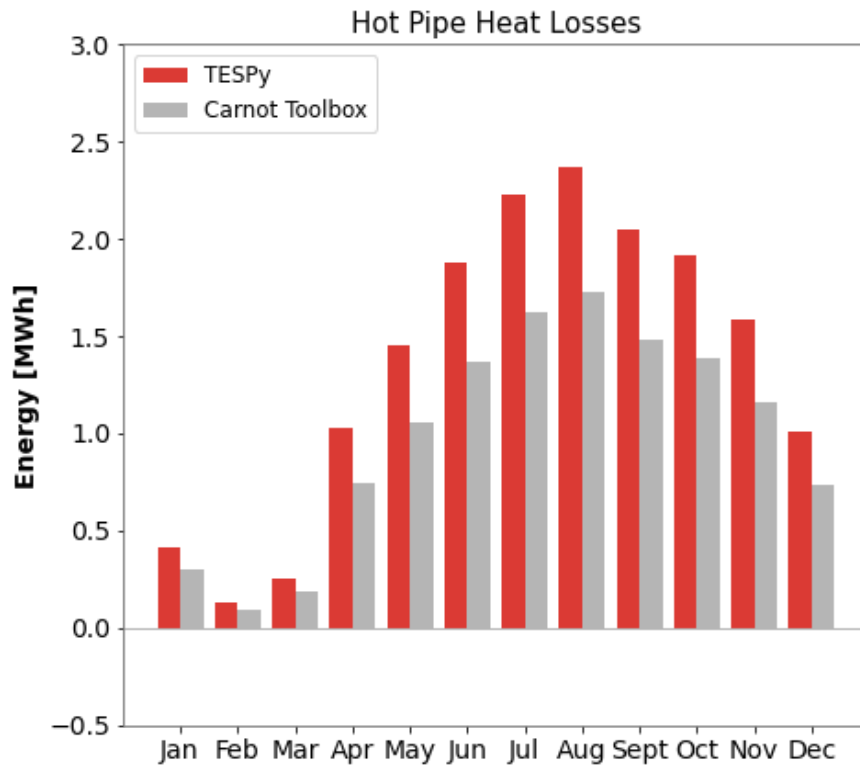


FIGURE 1.3: Heat losses calculation for the dynamic and steady state approach under low temperature conditions, ENaQ, from [7]

determined by the equivalent pipe length of the regarded network pipeline which simplifies the analysis neglecting the thermal inertia as well as the axial heat diffusion of the pipes, and as described by Van der Heijde et al. [9], at lower mass flow conditions parameters such as the axial heat diffusion, the pipe's wall friction and thermal inertia should not be neglected.

This master thesis compares the suitability of thermal quasi-steady state approaches with fully dynamic models spatially discretized with multi-nodes for modelling the performance of the network, considering all the aspects mentioned above. The performance of different modelling approaches is characterized in different network setups and operating conditions by comparing the simulation results with measurements.

Then, to accomplish that, the same simulation tools TESPpy and Carnot Toolbox are used, but this time applying a process of aggregation called the node method [10], which due to its formulation contemplates the axial heat diffusion and the thermal inertia. The analysis is done under different flow regimes and temperature levels,

finally the accuracy is validated comparing the results from the simulations with real data from an active district heating network.

**Main research question**

What is the effectiveness of dynamic and steady state models in accurately simulating heat networks through a space-discrete approach, considering different flow conditions and temperature levels?

**Specific questions**

- How to define a suitable number nodes to divide a pipe in several nodes for a spatial discrete analysis?
- What is the influence of different temperature's levels and mass flow regimes over the heat losses and outlet temperature?
- How does each input parameter impact the losses and outlet temperature?
- How does varying temperature levels and mass flow regimes affect the outcomes of single and multi node models?
- What factors influence the selection of either a steady state or dynamic approach for analyzing a district heating network?

## Chapter 2

# Theory

### 2.1 District heating networks modelling

District heating networks (DHN) are centralized heating systems that distribute heat from a source to multiple consumers via a network of pipes [11]. These systems provide a more efficient and environmentally friendly way of heating buildings compared to individual heating systems [11], from the creation of the concept in 19<sup>th</sup> century until now, there are 4 generations where each one was improving issues related to the security, fluid temperature levels and materials with poor thermal efficiency among others, the 4<sup>th</sup> generation seeks to follow the Net Zero emissions for 2030 with even lower temperatures, reduction of the GHG and decentralization of heat sources [12].

DHN operates in both hot and cold network temperatures [13] and can be modeled using either steady state or dynamic approaches. The accurate modelling of DH networks is important because it affects the performance, specially on those fed by RE such as collector or heat pumps [14]. As RE systems often operate at low temperatures the outlet temperature of DH networks is a key parameter that determines the efficiency, then an accurate modelling of the outlet temperature is essential to ensure optimal performance, reduce energy losses, and improve the overall efficiency of the system [15] [16].

Heat modelling gain major importance when the DHN is large and the total demand profile at the end-users is different than the total load profile at the plants. This means that the performance achieved might be significantly different depending on the position (and characteristics) of the energy sources and end-users [14].

Both modeling approaches are used to simulate the behavior of DHN. In steady state modeling represented by TESP<sub>y</sub>, the system is assumed to be in a uniform state, with

constant parameters such as temperature, mass flow, and ambient temperature, the ambient temperature of a buried pipe is the temperature of the soil. Steady-state modeling is useful when analyzing the system's behavior under different operating conditions that may not vary in function of time [17].

Counterwise of dynamic modeling, such as those in the MATLAB modelling tool CarnotTB [18], where the system's parameters are allowed to vary over time, and the behavior of the system is simulated under different time base conditions. Dynamic modeling is useful when analyzing the response of the system to changes in varying operating conditions [19].

## 2.2 Steady state approach, TESPpy

Thermal Engineering Systems in Python (TESPy) is an open-source software library for modeling and optimizing thermal power systems. It provides a flexible framework for building models of various energy systems [20], including DHN which is the one selected for the work, specifically the pipe component.

The Bernoulli equation, thermal resistance equation, and energy balance equation are essential equations used to model the pipe component in TESPpy

The pipe component is the crucial element in the DHN here, additionally to the Bernoulli equation 2.1, pipe's thermal behavior equation 2.2 and the rate of heat transfer through the pipe  $Q$  are essential equations used to model it. The main method to solve the system of steady state equations is with the iterative algorithm Newton-Raphson method, equation 2.4, as follows:

$$p_1 + \frac{1}{2}\rho v_1^2 + \rho g h_1 = p_2 + \frac{1}{2}\rho v_2^2 + \rho g h_2 \quad (2.1)$$

where  $p$  is the pressure,  $\rho$  is the fluid density,  $v$  is the fluid velocity,  $g$  is the gravitational acceleration, and  $h$  is the elevation.

$$Q = \frac{\Delta T}{R_{th}} \quad (2.2)$$

where  $\Delta T$  is the temperature difference between the inside and outside of the pipe.

The energy balance equation 2.3 is used to calculate the temperature of the fluid flowing through the pipe. The energy balance equation can be written as:

$$\dot{m}c_p(T_2 - T_1) = Q \quad (2.3)$$

where  $\dot{m}$  is the mass flow rate of the fluid,  $c_p$  is the specific heat capacity of the fluid,  $T_1$  is the inlet temperature, and  $T_2$  is the outlet temperature.

$$x_{i+1} = x_i - \frac{f(x_i)}{f'(x_i)} \quad (2.4)$$

This is the Newton-Raphson equation, where  $x_i$  is the current estimate of the root,  $f(x_i)$  is the function evaluated at  $x_i$ , and  $f'(x_i)$  is the derivative of the function evaluated at  $x_i$ . The method is iterative, which means that it uses the previous estimate to compute the next one.

The Newton-Raphson method is the iterative algorithm used in TESPpy to solve the non-linear system of equations. It is used to update the variables in the system until the residual is below a certain threshold, indicating that the solution has converged.

### 2.3 Dynamic approach, CarnotTB

The Conventional And Renewable eNergy systems OpTimization Blockset, from now on wards CarnotTB, is a software tool that is designed for the simulation, optimization and control of energy systems. It is based on the MATLAB, Simulink and is used to model conventional and renewable energy systems. The CarnotTB is specifically designed to optimize energy systems by improving efficiency, reducing cost, and minimizing environmental impact **carnotTB\_FH**:

The most interesting feature for this master thesis its ability to model district heating networks. CarnotTB takes into account the time-varying nature of the system. This is important because district heating networks are highly dependent on the weather conditions and the energy demand of the buildings that are connected to the network [19] [18].

As well as TESPpy, the crucial component is pipe, in this toolbox the pipe already includes the isolation. The isolated pipe component equations are based on the conservation of energy and the conservation of mass. CarnotTB's equation 2.5 takeS into account the flow rate of the water, the temperature of the water, and the heat transfer coefficient of the pipes.

$$\frac{c_{\text{wall}} L}{V_{\text{node}}} \frac{dT}{dt} = \frac{UA_{\text{loss}}}{V_{\text{node}}} (T_{\text{amb}} - T) + \frac{\lambda}{dx^2} (T_{\text{last}} + T_{\text{next}} - 2T) + \frac{\dot{m}c}{V_{\text{node}}} (T_{\text{last}} - T) \quad (2.5)$$

The left-hand side of the equation represents the thermal inertia that is the rate of change of the temperature of the pipe wall with respect to time. This is given by the product of the heat capacity of the fluid as well as the pipe wall with the term ( $c_{\text{wall}}$ ), the length of the pipe ( $L$ ), and the derivative of the temperature of the pipe wall with respect to time ( $\frac{dT}{dt}$ ).

The first term on the right-hand side of the equation represents the rate of heat losses from the pipe to the surrounding environment. This is given by the product of the overall heat transfer coefficient ( $UA_{\text{loss}}$ ), which takes into account the thermal conductivity and heat transfer coefficient of the pipe and the surrounding environment, and the difference between the ambient temperature ( $T_{\text{amb}}$ ) and the temperature of the fluid flowing through the pipe ( $T$ ).

The second term on the right-hand side of the equation represents the axial heat diffusion. This is given by the product of the thermal conductivity of the pipe ( $\lambda$ ), the inverse square of the distance between nodes ( $dx^2$ ), and the difference in temperature between nodes ( $T_{\text{last}} + T_{\text{next}} - 2T$ ).

The third term on the right-hand side of the equation represents the heat transfer through convection of the fluid forced to flow in the pipe direction. This is given by the product of the mass flow rate of the fluid ( $\dot{m}$ ), the heat capacity of the fluid ( $c$ ), the inverse volume of the node ( $\frac{1}{V_{\text{node}}}$ ), and the difference in temperature between the fluid and the pipe wall ( $T_{\text{last}} - T$ ).

In overall, first term is the *thermal inertia*, that represents the amount of heat that is stored in the pipe wall and is transferred to the fluid flowing through the pipe. The second term represents heat losses from the pipe to the environment. Third term is the axial heat diffusion, that represents the conduction given by central differences, the amount of heat that is transferred between nodes in the pipe. And the fourth and last term is the convection, representing the flow temperature propagation between the fluid and the pipe wall [18].

## 2.4 Discretization methods

Discretization is a fundamental step in numerical methods for solving partial differential equations (PDEs). It involves dividing a continuous domain into a finite number of discrete elements or nodes. These elements can then be used to approximate the solution to the PDE [21].

There are various methods for discretization, including finite difference, finite volume, and finite element methods. Each method has its own advantages and disadvantages, and the choice of method depends on the specific problem being solved [22].

Finite Difference Method (FD): The FD method involves approximating the derivative of a function using finite differences. The derivative is approximated by taking the difference between two neighboring points on the function. The first derivative of a function  $f(x)$  can be approximated by the following FD equation 2.6:

$$\frac{df(x)}{dx} \approx \frac{f(x+h) - f(x)}{h} \quad (2.6)$$

Where  $h$  is the distance between two neighboring points. This approximation becomes more accurate as  $h$  becomes smaller [22].

Considering the heat equation 2.7, the FD method can be used to discretize the spatial and temporal domains of a PDE:

$$\frac{\partial T}{\partial t} = \alpha \frac{\partial^2 T}{\partial x^2} \quad (2.7)$$

Where  $T$  is the temperature,  $t$  is time,  $x$  is position, and  $\alpha$  is the thermal diffusivity. This equation is used by CarnotTB for spatial discretization using the following FD equation:

$$\frac{T_i^{n+1} - T_i^n}{\Delta t} = \alpha \frac{T_{i+1}^n - 2T_i^n + T_{i-1}^n}{\Delta x^2} \quad (2.8)$$

Where  $i$  is the index of the discretized position,  $n$  is the index of the discretized time,  $\Delta t$  is the time step, and  $\Delta x$  is the position step.

A fellow discretization equation is 2.9, that is used mainly in the definition of the optimal number of nodes in section 3.2.



$$\frac{k_e (T_E - T_P)}{(\delta x)_e} - \frac{k_w (T_P - T_W)}{(\delta x)_w} + \bar{S} \Delta x = 0 \quad (2.9)$$

This equation represents the heat transfer balance for a control volume, where  $T_P$  is the temperature at the center of the nodes,  $T_E$  and  $T_W$  are the temperatures at the east and west sides, respectively. The term  $(\delta x)_e$  and  $(\delta x)_w$  represent the distance between the center of the control volume sides, respectively. The values of  $k_e$  and  $k_w$  is the thermal conductivity at both sides, respectively. The term  $\bar{S}$  represents the volumetric heat source term, and  $\Delta x$  is the size of the control volume. The description of the terms is taken directly from Patankar 1980, chapter 3, [22].

The FD method can be used to solve both linear and nonlinear PDEs. In the case of nonlinear PDEs, the FD equations are solved using an iterative method, such as the Newton-Raphson method also utilized by TESPpy in equation 2.4, [18], [17], [22].

This method has several limitations that need to be considered when it is used for solving PDEs. One limitation is that it can only approximate the solution at the discrete points, then the accuracy of the solution depends on the step size used for discretization, and the solution may be inaccurate if the step size is too large [23], [22].

In general, FD method calculate the derivative of a function using finite differences [22]. The method can be used to discretize both the spatial and temporal domains of a PDE, and it can be used to solve both linear and nonlinear PDEs [21]. Those limitations and challenges associated with the method, including the selection of the optimal step sizes, be discussed in the results section of this master thesis.

## Chapter 3

# Methodology

The study aims to evaluate the accuracy of quasi-steady state and dynamic models, incorporating thermal inertia, axial heat transfer across a range of input temperature and mass flow levels. Therefore, two scenarios are presented in table 3.1 each one in one column.

For both scenarios is displayed the approach; Dynamic or Steady state, the software: CarnotTB and/or TESP<sub>y</sub>, and the two proposed simulations.

the comparison of the proposed simulations must be read from top to the bottom inside of the column of the scenario, each scenario compares simulation 1 against simulation 2.

TABLE 3.1: Description of the two scenarios analyzed, defining for each one the approach, software and proposed simulations comparing the models

Project-Scenario	ENaQ	Lampoldshausen
<b>Approach-Software</b>	Dynamic/CarnotTB	Steady state and Dynamic / TESP <sub>y</sub> and CarnotTB
<b>Simulation 1</b>	1 pipe, no discretization <b>1 pipe, 1 node</b>	Several pipes, no discretization <b>Multi pipes, 1 node</b>
<b>Simulation 2</b>	1 pipe, discretized in several nodes <b>1 pipe, multi nodes</b>	Multi pipes, different discretization for each one <b>Multi pipes, multi nodes per pipe</b>

To fully understand the table 3.1, a detailed description of each scenario and its corresponding simulations is provided. This includes a description of the project associated with each scenario, an explanation of the method used for spatial

discretization, and a comprehensive definition of each proposed simulation. Additional information about scenario 1 and 2 are presented in appendix 6.1 and 6.2

## 3.1 Projects description

The name of each scenario is inherited from the name of the project from where the analyzed data comes from, ENaQ and Lampoldshausen.

The selection of these two projects was based on their differing operating conditions, network sizes, and demands, resulting in varying flow regimes and temperature levels, as stated in the theses title. This ensures the inclusion of diverse data and parameters for analysis.

For each project, which will also be referred to as *scenarios* henceforth, a general description will be provided, along with an explanation of the selection process for their specific information and the exact boundaries utilized.

Scenario ENaQ is the first one to be described due to its size and protagonism in several previous studies such as [7], [8].

### 3.1.1 Scenario ENaQ

The name stands for *Energetic Neighbourhood Oldenburg Air Base*, is a climate-friendly project that looks for cover the total neighborhood demand mostly by locally generated energy, under the concept "energetic neighbourhoods" where the producers and consumers are located close to each other, connected by the same network and communicated by a community portal to know, within others, information on the current status of energy generation, energy consumption and internal energy trading [24].

This living lab has the task of developing and researching the overall energy concept to map the diversity of all components of a smart grid over three important pillars; *Technical* that should guarantee the greatest possible energy efficiency, *Digital* with the platform that enables intelligent load and procurement management for energy producers and consumers, and the last pillar *Participatory* where the citizens of Oldenburg are involved in order to meet their needs, wishes and interests in the planning and implementation of the climate-neutral residential quarter [25] [26] [27].

There are several previous studies using ENaQ data to specifically analyze its heat network, the two most interesting studies for this master thesis were both developed in the DLR Institute of Networked Energy Systems.

The first one was done in 2020 under the name "Technology Pathways for transforming High Temperature to Low Temperature District Heating Systems in the ENaQ Project" [8] this study was also comparing ENaQ HTDH against the district heating network named TUM, utilizing the dynamic software CarnotTB, one of the key conclusions was CarnotTB is suitable for conducting thermal behavior analysis for district heating, however some assumptions were done, specially with ENaQ data because the scope of CarnotTB cannot afford such a detailed synthetic data from network infrastructure and specific heat demands.

From the aforementioned work, the whole carnotTB model was taken and simplified such that only three primary inputs are needed: mass flow [kg/s], inlet temperature [°C], and soil temperature [°C] as presented in figure 3.1 These are the minimum input parameters to feed pipe inlet in the simulations, and get as outcome a pipe outlet temperature [°C] and energy losses [Wh] which is the main result to perform the analysis and comparison between simulations.

The final model is presented in figure 3.1, the figure is split in three purple areas: *Inputs*, *Process* and *Results*. *Inputs*, the first one, is where the three main inputs are feed, first is the soil temperature generated by a sine wave generator, and in orange are inlet temperature and mass flow, provided by files in *.csv* format. The second purple area *Process*, contains the CarnotTB blocks, in yellow is the thermo-hydraulic bus which transform the inputs in variables to be processed by the pipe with isolation thickness, the pipe is the blue block following thermo-hydraulic bus. As described in the theory, pipe is the most important element in the simulations, here is where criterion like geometry, thermal and hydraulic are set up.

The last purple area *Results*, is where the outputs are delivered and saved.

Figure 3.1 depicts all the pipes in the ENaQ network as a single equivalent pipe, similar to the approach adopted by Duran and Maldonado [8], [7].

The data used for the ENaQ network is synthetic and obtained through simulations that emulate the real system's size, supply, and demands. The data covers a period of one year with a timestamp of one hour, and the three primary inputs in table 3.2 are:

Mass flow data set is from 0 to 9.000 kg/h following the residential heat load profiles, which means low demand in the night and high demand in the day, also a seasonal

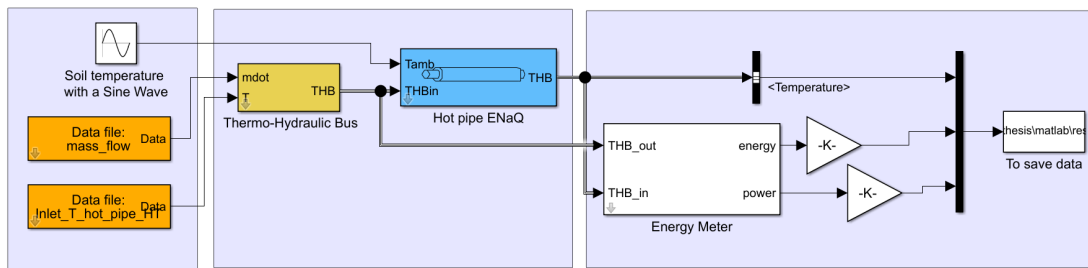


FIGURE 3.1: Simplification of CarnotTB model from [8], to spatially discretize the pipe, ENaQ

trend with low mass flows in summer and high in winter. The inlet temperature is from 70 to 78,9 °C, the variation thorough the year is quite constant because of the heat storage supply and a CHP, which consistently provides high supply temperatures.

Finally, The soil temperature is determined by a sinusoidal waveform that completes a full cycle in a year, with temperatures ranging from 2 °C during winter to 13 °C during summer.

ENaQ data is primarily used in this master thesis to test the differences between single and multi-node models, mainly due to there are not real data to compare the accuracy, contrary to the next scenario.

### 3.1.2 Scenario Lampoldhausen

Lampoldhausen is a research centre of space propulsion with more than 57 years of history developing sustainable propulsion technologies with unique test stands and plants for the testing of the components to propulsion testing up to the testing of entire rocket stages. DLR's aerospace village Lampoldshausen site is located 25 kilometres north of Heilbronn, in northern Baden-Württemberg, Germany. The site accounts for 51 hectare fully connected by networks constantly controlled and monitored [28], one of those is the integrated heating network whose information was chosen and filtered for the purpose of this research.

In figure 3.2 is shown the map of the entire aerospace center, but due to it is a research institute there are many buildings with particular water and heat demand, then a specific part of the network was selected being careful to keep in the new filtered branch enough thermal gradients and pipe characteristics.

The selected branch are the colored lines over the main pipeline including the buildings that are marked in yellow, in figure 3.2 the branch starts, from left to right,

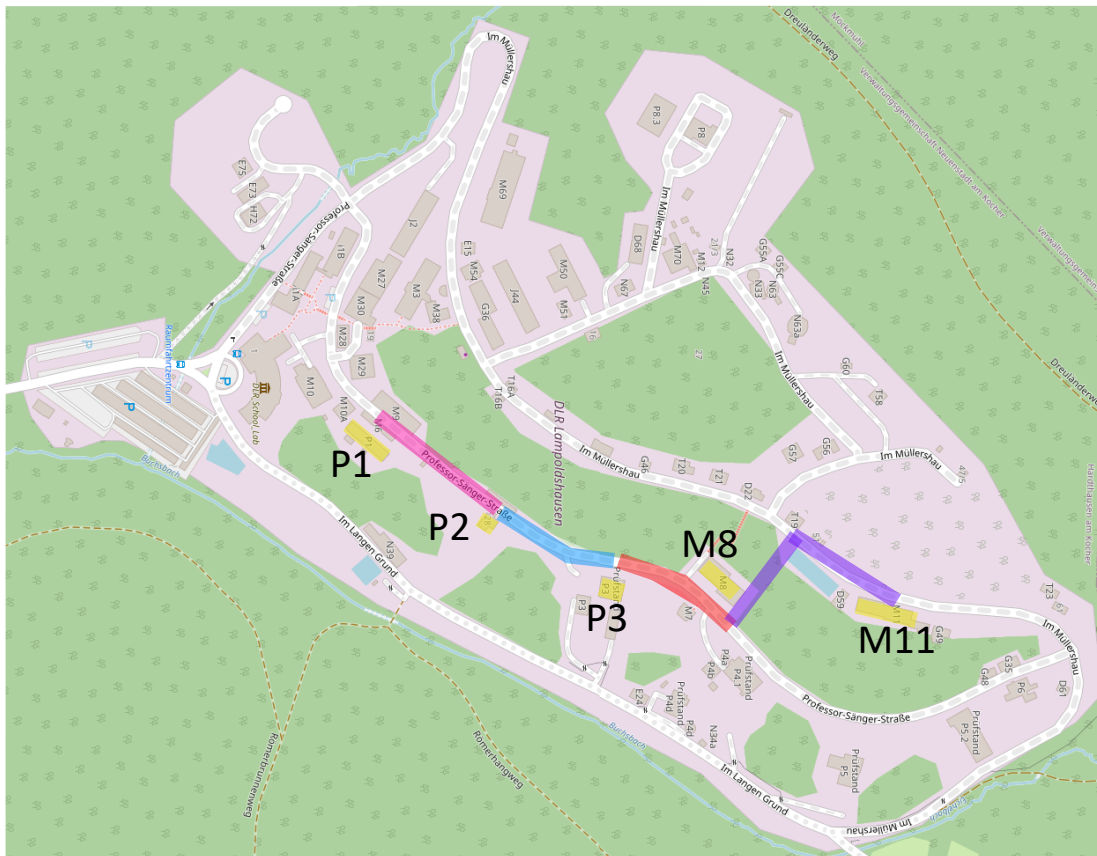


FIGURE 3.2: Complete aerospace center, and selected branch of heat network to study marked in colors, Lampoldshausen, modified from [29]

in the fork of the building tagged as P1, and pass by the forks of building P2, building P3, M8, M11, and finalizes directly in the building M11.

The first assumption is the real inlet temperature and mass flow recorded in the fork of building P1 are the initial parameters, second assumption is the soil temperature is fixed as a constant value of 12°C due to is not provided in the measured data. Third assumption is considering there are not losses in the pipes going after the forks directly to the buildings, apart from the main pipe between the forks, only the pipe connecting building M11 is considered, the mass flow and outlet temperature arriving to M11 are the outcomes that will be compared with the simulations.

Fourth and last assumption is even when the network has hot pipe for heat supply and cold pipe for water return, the scope of the thesis is limited only to the supply hot pipe.

It is noteworthy that in order to calculate temperature gradients only building M11

is simulated, but all buildings the other buildings are represented in the simulations as sinks, where mass flow is diverted in order to deliver the corresponding final real mass flow that comes from P1 to M11.

Having selected the branch, the next step is to simulate it first in TESP<sub>y</sub> and later in CarnotTB. As TESP<sub>y</sub> was modelled first, it was calibrated for January to accurately reflect the behavior of the network under those specific conditions. TESP<sub>y</sub> simulation was done by defining the network characteristics like type of fluid, physical characteristics of the pipes, their connections and inclusion of complementary network elements such as sources, sinks, heat exchangers, pumps, valves, merges and splitters, as well as measurement units for pressure, temperature and mass flow which are the same from ENaQ to be able to compare both scenarios. The complete setup of the network in TESP<sub>y</sub> was done following the documentation and examples provided by TESP<sub>y</sub> [17].

Later, CarnotTB simulation was done following the same principle of ENaQ, as it is presented in figure 3.3

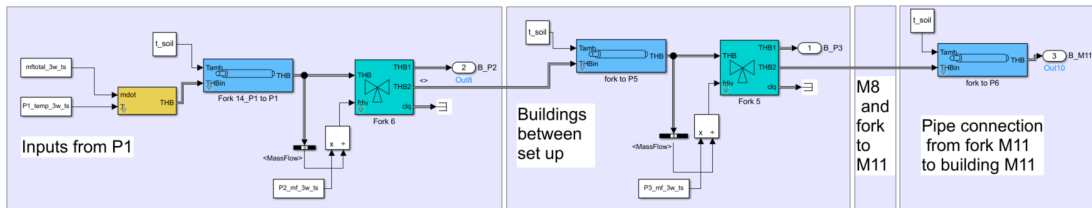


FIGURE 3.3: Selected branch of Lampoldshausen heat network, in CarnotTB simulation

There are four purple areas, the first one is where the simulation starts and is fed by the three white rectangles representing mass flow and inlet temperature, as well as the white square feeding the soil temperature as a constant, the yellow and blue rectangles are the CarnotTB blocks which deliver the resulting temperatures to the clear green valve that diverts the mass flow between the next building and the continuation of the main pipe.

The second purple area is the representation of how the next building is connected and configured. Third block just represents that the same is done for the remaining buildings until reach the pipe which connects the fork M11 with the building M11, where the outlet variables are taken to do the comparison with the TESP<sub>y</sub> and real data. This is how the single node simulation was done.

TABLE 3.2: Summary of input data and parameters for ENaQ and Lampoldshausen

Projects data	Lampoldshausen					EnaQ		
Pipe name	P1	P2	P3	M8	M11	1 equivalent pipe		
Length [m]	144,1	120,3	80,3	35,8	221,2	32,83		
Diameter [m]	0,11	0,11	0,11	0,11	0,04	0,04		
Ka [W/K]	220	220	15	40	140	97,92		
Thickness [%]	8,95	7,36	141,9	12,63	24,37	NA		
Parameters	Max	Min	Range		Max	Min	Range	
Soil temperature [°C]	12	12	0		13,79	2,2	11,5	
Mass flow [kg/h]	2.44	4.931	2.491		9	0	9	
Inlet temperature [°C]	72,6	51,8	20,8		78,9	70	8,9	

The provided Lampoldshausen real data last for one year and has a timestamp of 15 minutes, much more detailed than ENaQ. Therefore, only one week per month in the first quarter of the year is considered for the investigation. Although this is a small portion of the data, three weeks of information are sufficient to determine whether the simulation results match the measured data.

Lampoldshausen boundaries are:

Mass flow data set is from 2.440 kg/h to 4.931 kg/h with no residential daily nor seasonal behavior as ENaQ due to it is a testing centre and not households. The inlet temperature is from 51,8 °C to 78,9 °C, the variation cannot be defined as constant because the inlet temperature is assumed by adapting the data from the building P1 which is not a real heat supply. Finally, the soil temperature as mentioned before is not provided, then it is fixed to 12 °C constant, refers to table 3.2.

Lampoldshausen data is used in this master thesis primarily to test the accuracy between real data and models, and this is the main difference with scenario ENaQ.

A summary of the aforementioned data for both projects is presented in table 3.2.



At glance, by comparing the data from both projects in table 3.2, there are 3 important observations: first, ENaQ mass flow range is much more bigger than Lampoldshausen mass flow by 6.500 kg/h. Second and opposite, the variation of the inlet temperature is bigger for Lampoldshausen with a range of 20 °C against the 9 °C variation range from ENaQ, and last but not least, the soil temperature from ENaQ has a yearly sinusoidal shape with 11 °C range while for Lampoldshausen it is constant in 12 °C.

## 3.2 Method to discretize the models

### Optimal number of nodes

The configuration of models in figure 3.1 and figure 3.3 were designed to be suitable to analyze it in single and multi nodes, also flexible to change the input parameters as it will be described in the simulations performed for each scenario at the end of this section.

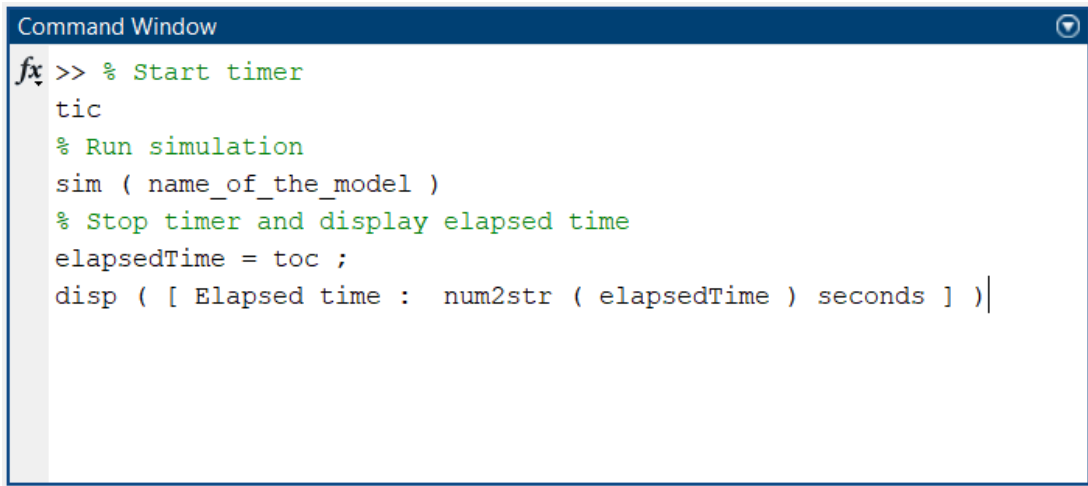
The discretization method is selected following Patankar [22] four basic rules. Rules that must be consider to select the method of deriving the discretization with the FD equations 2.6. First one is the consistency at control-volume faces, the heat flux that leaves one node must be identical to the flux that enters the next node, and this is respected if one single pipe is divided and analyzed individually but preserving the same physical and thermal attributes such as the thermal conductivity  $kA \frac{W}{K}$ , length, diameter and thickness percentage like are described for the pipes in the table 3.2.

Second rule is positive coefficients, the coefficients from each node should be positive for neighbor nodes, however the same source [22] indicated there are numerous formulations that frequently violate this rule, as well as the third rule that seeks to have a negative slope in the linearization of the nodes, but this is an ideal physical process that becomes arbitrary in this research due to the utilized amount of variables, but is essential for more detailed analysis where instabilities and physical unrealistic solutions arise because they have more detailed data input.

The fourth and last rule is the sum of neighbor coefficients, that implies the temperature of a node center-point is a weighted average of the neighbor values, for both scenarios in this research the rule is true due to the source term  $T$  in equation 2.6 is never absent, and the temperature boundary increases proportionally to the increment of the source.

In order to define the number of nodes, first the six simulations from ENaQ: 1n, 5n, 10n, 20n, 40n and 80n, where "n" states for "node", are done as presented in figure

3.1. Each one of the mentioned simulations were perform individually, and for each simulation the complementary code in MATLAB is run with the main script 3.4 in parallel, to register the time taken by the software, presented in column 5 of table 4.1:



```

Command Window
fx >> % Start timer
tic
% Run simulation
sim ( name_of_the_model )
% Stop timer and display elapsed time
elapsedTime = toc ;
disp ( [ Elapsed time : num2str ( elapsedTime ) seconds ] )

```

FIGURE 3.4: Matlab code to register the time taken by the software solving the simulations, for ENaQ and Lampoldshausen

Later, for each simulation the Root Mean Square Error (RMSE) was calculated, RMSE is a measure of the goodness of fit of a linear and no linear regression model, it is commonly used to compare the performance of different models as explained in [30]. Equation 3.1 from [30] is:

$$RMSE = \sqrt{\frac{\sum_{i=1}^n (y_i - \hat{y}_i)^2}{n}} \quad (3.1)$$

where  $y_i$  are the results from 1n,  $\hat{y}_i$  are the results from the other six space discrete simulations, and  $n$  is the number of data points analyzed.

Care must be taken in the interpretation of the RMSE magnitude, due to in ENaQ the reference model is the simulation 1n, while in Lampoldshausen the real data is the reference. The correct interpretation will be explained in detail for each scenario in section 4.1.

Due to there are not enough documentation of how to split pipes in a DHN for a spatial discrete simulation, but still taking into account the conclusions from [23] and [22], the best trade-off was achieved for ENaQ with nodes of 20 % of total pipe length as explained in table 4.1. Then the same was done for Lampoldshausen discretized models, in total there are two discretized models, one following the 20 % method

named *Disc*, and second simulation *Disc x3* that double the number of nodes from *Disc* to verify the accuracy between models, this is better explained in table 4.2.

But as rule of thumb, mainly the simulations with 20 % of the total pipe per node were used for the presentation of the results and comparisons, this means the models named *5n* in ENaQ and *disc* in Lampoldshausen.

### CarnotTB pipe settings

The most important task to develop a fair and correct comparison of models rely on the setup of the software. TESPpy setup is quite straight forward following the documentation provided by the same Python library [17], it should be clarified this software and its documentation are being constantly updated and there are meaningful examples for help.

However, is not the same for the library CarnotTB, which last update was done in 2018, but as the components operates in the same way as components in Simulink MATLAB, and MATLAB is a private software fully maintained, the configuration of the models are supported by Simulink help desk.

In figure 3.5 is presented the setting box with four windows to setup the isolated pipe in CarnotTB, each window requires for specific information as follows:

- Geometry, window A: Here physical characteristics are fed, as the outer diameter and total length of the pipe in meters, the difference in static height is 0 m due to the pipe networks from both projects are underground, then pressure is not considered.
- Thermal, window B: This window contains the most complex parameters and must be carefully defined.

Isolation thickness in % (100%: isolation thickness = diameter, minimum 1%): This is a parameter that is not provided with the real data, then, from the explanatory paragraph in the head of the box is known CarnotTB uses the equation of heat transfer coefficient per unit length  $ul$ , but here CarnotTB expects to account with values from inner diameter and it was also not provided with the real data, for this reason is necessary to re-arrange the equation to find out the isolation thickness in % utilizing the available data. First, taking as pillar the normalized heat transfer equation 3.2 and replacing the term  $U$  by the overall heat transfer coefficient for a cylindrical heat transfer surface the equation.

The normalized heat transfer equation is taken as pillar, then the term  $U$  is replaced by the overall heat transfer coefficient for a cylindrical heat transfer surface as it can be seen in 3.2, this ensures that the equation can be solved with the supplied values.

$$U \cdot d \cdot L = K_a \implies \frac{2\pi\lambda}{d \ln(d_i/d_o)} \cdot d \cdot L = K_a \quad (3.2)$$

Where  $U$  is the overall heat transfer coefficient that is replaced in the right side,  $diam$  is outer diameter of the pipe,  $L$  is the length of the pipe,  $K_a$  is the overall thermal conductivity. In the right side are the terms  $lambda$  that is the pipe thermal conductivity which was setup in 0,04 W/mK as a generic low value due to the insulation of the pipes, and  $ln$  natural logarithm of  $d_o$  the inner diameter of the pipe, over  $d_i$  the inner diameter of the pipe that is the only unknown parameter. The next step is to clear the Neperian of diameters from the rest of the terms since it represents the isolation thickness, as result the final equation 3.3 is presented, always controlling the units of the equation with dimensional analysis.

$$\ln\left(\frac{d_i}{d_o}\right) = \frac{2 \cdot \pi \cdot \lambda \cdot d \cdot L}{d \cdot K_a} \implies \frac{d_i}{d_o} = \exp\left[\frac{2 \cdot \pi \cdot \lambda \cdot d \cdot L}{d \cdot K_a}\right] \quad (3.3)$$

Then, the equation is applied for each pipe to find out their individual isolation thickness in the case of Lampoldshausen, and applied only once in ENaQ because there is only one pipe. Last step is normalize the value in percentage as it is required by the setting box.

Effective conductivity in the pipe is a parameter that is only required for spatially discretized models, in figure 3.5 is 0 because is a single node model, but multi nodes models it was set up in 0,598 W/mK which is the thermal conductivity of the water under standard conditions.

The capacity of pipewall per length is fixed in 1.000 J/(mK) as an average value due to the pipe materials in the network may be different between them, too high or low values could lead to inefficiencies in the system. And finally, the initial temperature is given as a starting point from where the system can calculates the losses. This requirement is fed with the highest inlet temperature value achieved in the system.

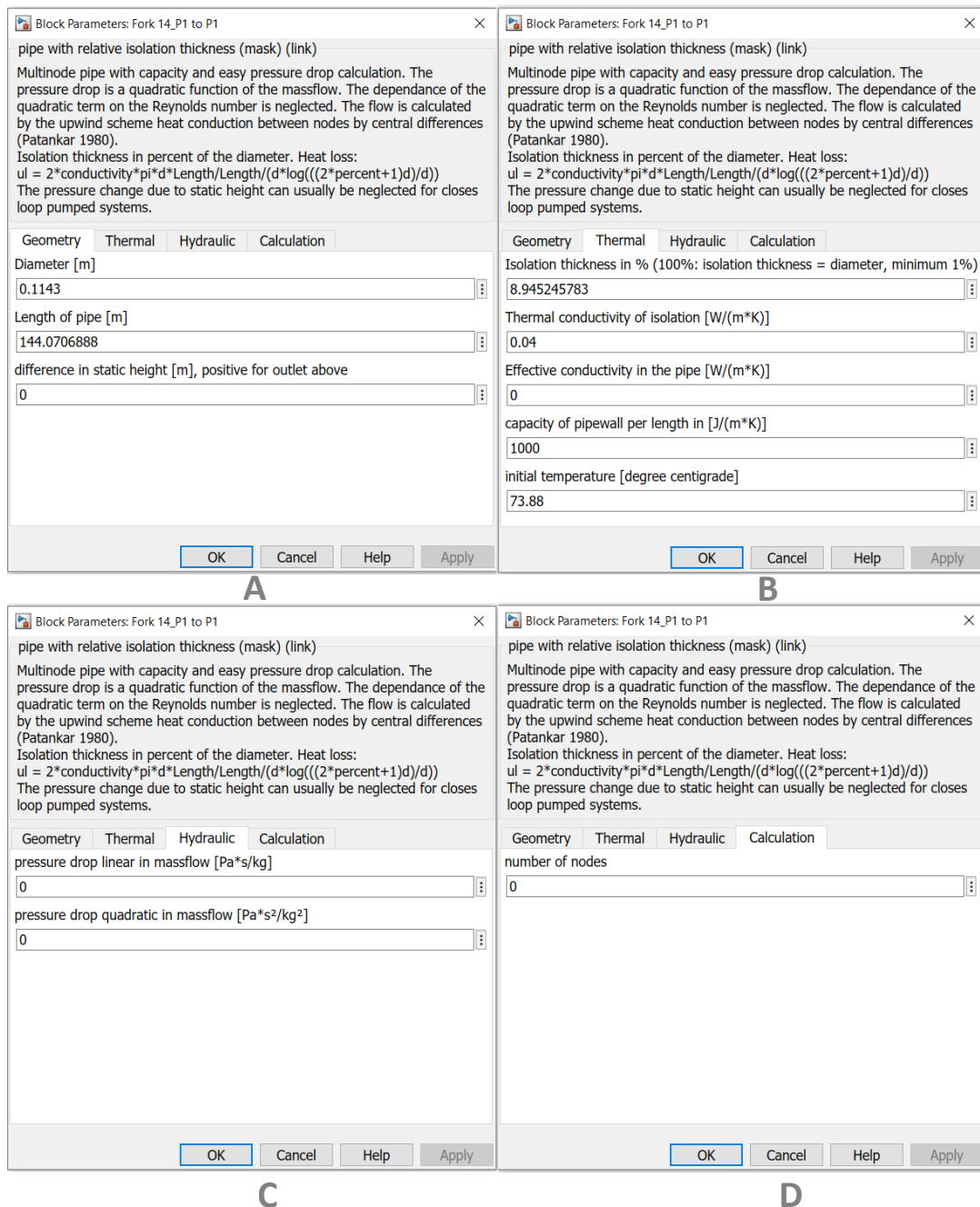


FIGURE 3.5: CarnofTB pipe block setup, from the main pipe fork P1 to fort P2, Lampoldshausen

- Hydraulic, window C: As CarnofTB is a dynamic tool, complementary parameters can be provided to boost the complexity of the system, however, for this investigation pressure is not included and both parameters here required

can be setup in 0 without important affectations in the results.

- Calculation, window D: Refers to number of nodes into which the tube is divided, the number of nodes are explained in 4.1 and 4.2.

### Statistical tool for data visualization

Regarding the first presentation of the results such as energy losses and outlet temperatures for both scenarios, the statistical data visualization method named *Box and Whiskers* was utilized due to is a graphical tool used to summarize the distribution of a set of numerical data.

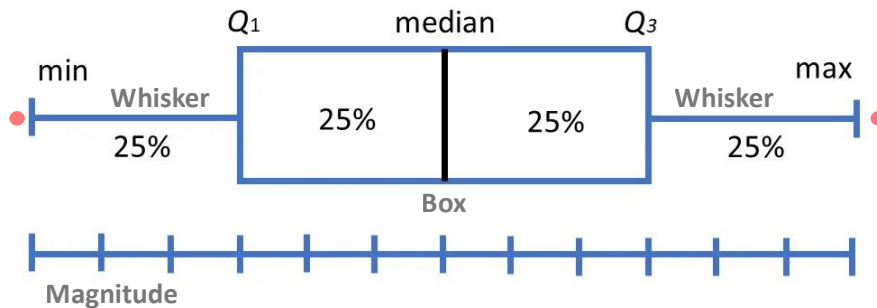


FIGURE 3.6: Box and Whiskers Statistical tool for data visualization, modified from [31]

The plot consists of several boxes as the box presented in figure 3.6. It shows the middle 50 % of the grouped data points with a line inside each box that represents the *median*, and whiskers that extend out from the box to show the minimum and maximum range of the data, each whisker represents 25 % summing up 50 % to complete the 100 % of the data.

The width of the box represents the spread of the data, between the lower quartile  $Q1$  and upper quartile  $Q3$ , wider boxes indicate greater variability. The whiskers show the range of the data outside the box, which means the other 50 % of the grouped data points, and outliers are plotted as individual red points at the extremes of the whiskers which are not part of the 100 % of the data. This tool can provide insights into the central data tendency, variability, and potential outliers [32], [31].

After the first results, several simulations are execute to investigate the influence of each input parameters, as described below.

### 3.3 Simulations

Recalling table 3.1, in the case of ENaQ, the simulation 1 named **1 pipe, 1 node** stands for simulation **1n** that is the model that contemplates the entire pipe in one single node. This model simulate the pipe as described at the end of section 3.1.1. Then, it is compared by the proposed simulation 2 named **1 pipe, multi nodes** that stands for all the simulations that include more than one node, i.e. 5n, 10n, 20n. Those simulations are done with the dynamic approach, which mean using CarnotTB. From the comparison of those two simulations is expected to identify the main factors influencing the differences between single and multi nodes models in the context of the dynamic approach.

In the case of Lampoldshausen, the simulation 1 named **Multi pipes, 1 node** stands for the model not discretized presented in 3.3, as the network already contemplates 5 different pipes it takes the name **Multi pipes**, but this model considers every single pipe of the network in one single node, receiving the second part of the name **1 node**. Then, it is compared by the by the proposed simulation 2 named **Multi pipes, multi nodes per pipe** that, as described before Multi pipes is because it has 5 pipes, and the **multi nodes per pipe** as its name indicates, each pipe will be considered into several nodes, this include the model *Disc* and *Disc x3* as explained at the end of the Lampoldshausen project description.

Additionally to the already mentioned simulations, there are further tests to confirm the weight of the effect of inlet parameters, because the results from proposed simulations, under certain conditions, were not fully exposing the reasons of the behaviors. Those further simulations are the following:

#### **Soil temperature**

Due to Lampoldshausen has a constant soil temperature, there was not data to contrast with ENaQ, then the white sine wave block generator from ENaQ setup, in figure 3.1, was changed for a block with a constant of 12 °C to induce the system to have more thermal gradients and check differences.

#### **Mass flow**

As mass flow has a strong effect in the differences achieved in ENaQ, even following the same shape, the mass flow was changed to have a lower operation range and a sinusoidal shape. To accomplish that the first orange box in figure 3.1 was changed by another white sine wave block generator providing values between 2.440 kg/h and 4.931 kg/h, that block was connected to the thermo-hydraulic bus, this is meant

to reduce the mass flow variation and check the new shape and magnitude of the differences.

### Inlet temperature

Part of the motivations for this master thesis is helping with the integration of the RE into the HN by reducing the inlet temperature to be LT, then, the networks heat supply can be provided solely with RE, getting rid of the fossil fuels.

The test is meant to simulate ENaQ under LT conditions. To do this a *synthetic profile* was designed and applied to the model, which means the model is fed with temperatures between 30 °C and 60 °C, then again a white sine wave block generator was implemented instead of the second orange box in figure 3.1, in that order is possible to compare Hot Temperature HT represented by the orange line versus LT represented by the blue line in figure 3.7, and check the differences with the RMSE method.

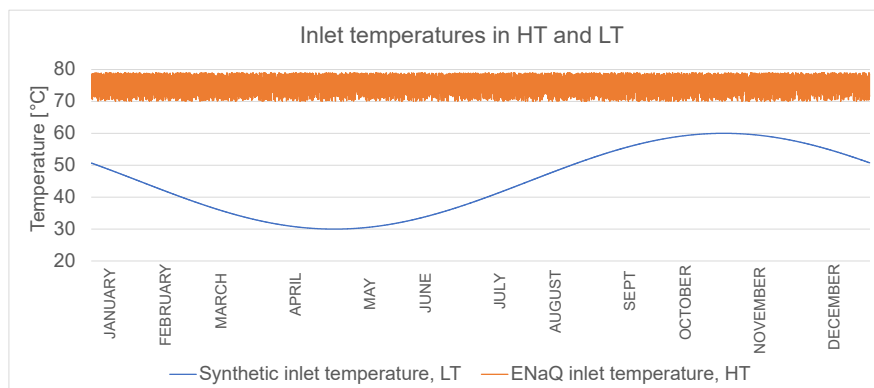


FIGURE 3.7: Range of operation of HT profile original from ENaQ, and synthetic profile for LT, comparison

### Increment of nodes in TESP<sub>y</sub>

Results from ENaQ single node in TESP<sub>y</sub> are not compared against CarnotTB due to the original model from Duran [8] in CarnotTB is simulating several components such as heat exchangers, pumps and cold pipes feeding-back the seasonal storage, and TESP<sub>y</sub> model from Maldonado [7] only analyzes two pipes, no additional components are included, then the outlet temperature and losses are calculated different for each model, which makes the comparison unfair. The offset between them is high even using the same input parameters because the original purpose for each one was different.



But still, a preliminary test was designed to check if the spatial discretization has some effect in the TESP<sub>y</sub> simulation from ENaQ. Then Maldonado's TESP<sub>y</sub> code was rewritten to split the pipes in  $3n$  and  $10n$ , and check if the results are affected and why.

## Chapter 4

# Results and Discussion

The description and discussion of the results are presented in parallel for both scenarios ENaQ and Lampoldshausen. The structure of the chapter sheds light on the two main research questions mentioned in section 1 to define a suitable number of nodes for a sound spatial discretization of the dynamic models and what is the effect of the axial heat transfer phenomena on the errors in different model operation.

First, is described the definition of number of nodes for a suitable spatial discretization for the dynamic model. And second, the effect of the axial heat transfer regarding each input parameter.

### 4.1 Definition of number of nodes

The optimal number of nodes to perform the spatial discrete models depends on the specific operation conditions and size of the system being analyzed and the level of detail required for the analysis.

both scenarios here analyzed require as input data: mass flow, initial temperature, pipe's materials, sizes and lengths. Specific heat capacity and axial heat transfer coefficients are additional requirements for dynamic models. As the amount of variables are considerable low, both scenarios can be considered as simplified systems [21], then studies like Haddou et al [23] can be applied.

Haddou et al [23], presented an study that investigated the optimal number of nodes for simulating the transient behavior of a plate heat exchanger. The study concludes that a relatively small number of nodes (around 10-15) were sufficient to simulate the heat transfer in the system with fair precision, while still having reasonable computational efficiency and time consumed.

To find the optimal number of nodes for scenario ENaQ, six simulations are done increasing the number of nodes from 5 to 80, and validating how far are the results from the reference with only 1 node, this deviation is measured with the Root Mean Square Error (RMSE), additionally in the next table 4.1 are also presented the length of the nodes.

TABLE 4.1: RMSE, length and duration of the software running for 1 year each simulation, in function of the number of nodes, ENaQ

Number of nodes	RMSE outlet temperature	RMSE energy losses	Length node [m]	simulation time [sec]
1n	0,000	0,000	32,83	4,57
5n	1,925	0,256	6,566	7,03
10n	2,242	0,294	3,28	7,94
20n	2,410	0,315	1,64	9,73
40n	2,678	0,348	0,82	12,36
80n	2,921	0,378	0,41	43,05

Haddou's study found that increasing the number of nodes led to higher accuracy but also increased computational cost, and the authors recommended using a trade-off between accuracy and computational cost to select the optimal number of nodes [23]. Considering that the simulation 1n is the reference in scenario ENaQ, the simulation 5n provides the lowest RMSE for both output variables with 1,95, which means 5n predictions are far enough to be able to find significant temperature gradients with the spatial discrete method. The length of each node is 20 % the length of the original pipe depicting to be a good sample with the lowest time consuming.

The 10n and 20n models will also be included in the analysis to evaluate the impact of the input parameters. However, the remaining models will not be considered further as the increase in the RMSE is not significant despite the substantial increase in the number of nodes. For instance, the increase in RMSE between the 1n and 5n models, with only four additional nodes is 1,925 °C, although the 80n model has 40 times more nodes than the 40n model and the RMSE increases only by 0,24 °c.

The conditions for scenario Lampoldshausen are different, there are five pipes with different length as described in methodology, the average length is 120 m. Then, based on the results from ENaQ a normalization is assumed with the Three Sigma Rule method.

Three Sigma Rule method states what is the proportional number of nodes for each pipe length whether for 32,83 m is needed 5 nodes. Then, for each pipe a specific

number of nodes is defined and presented in table 4.2.

TABLE 4.2: Definition of the optimal number of nodes based on ENaQ, for Lampoldshausen

Name	Length (1n) [m]	Nodes for spatial discretization (disc)	Nodes for threefold discretized (x3)
Fork 15 to building P2	144,07	22	66
Fork 16 to building P3	120,26	18	55
Fork 17 to building M8	80,28	12	37
Fork 18 to building M11	35,84	5	16
Building M11	221,17	34	101
Building P3	13,28	2	6

For Lampoldshausen the reference 1n is the CarnotTB model itself with each pipe analyzed with the real length, then the first spatial discrete model (disc) is equivalent to 5n, and finally the spatial discrete model (Disc x3) where each pipe is divided into 3 times the number of nodes from the first discretized model (Disc).

For a better understanding, from now on-wards, mainly the model 5n from ENaQ and the first spatial discrete model (disc) from Lampoldshausen are going to be used, additional models could be considered to deeply analyze the axial heat transfer effect and they will be properly mentioned and illustrated.

## 4.2 Differences in the results for ENaQ and Lampoldshausen

In this section the outlet temperature and energy losses from single and spatial discrete models are presented. First the results from ENaQ with one figure for each result, outlet temperature and losses due to the length of the data.

Later, a comparison of results between real data, single and spatial discrete models for Lampoldshausen scenario are presented in one comparative figure.

For both scenarios is used the statistical method for data visualization *Box and Whiskers* mentioned in the methodology, below each figure are the chart remarks and a detailed paragraph describing the findings.

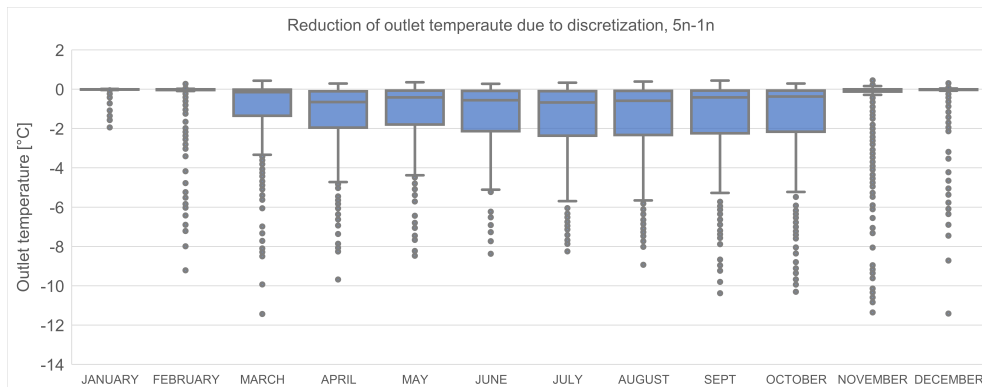


FIGURE 4.1: Reduction of outlet temperature due to spatial discretization for 1n - 5n, ENaQ

Chart remarks:

- more than 75 % of the data are below 0 °C.
- Differences rise up until 10°C for 11 of the 12 months of the year.
- From November to February the differences are extremely low, however the outliers ascent to 12 °C .
- From March to October the differences are bigger between models with a negative skew.

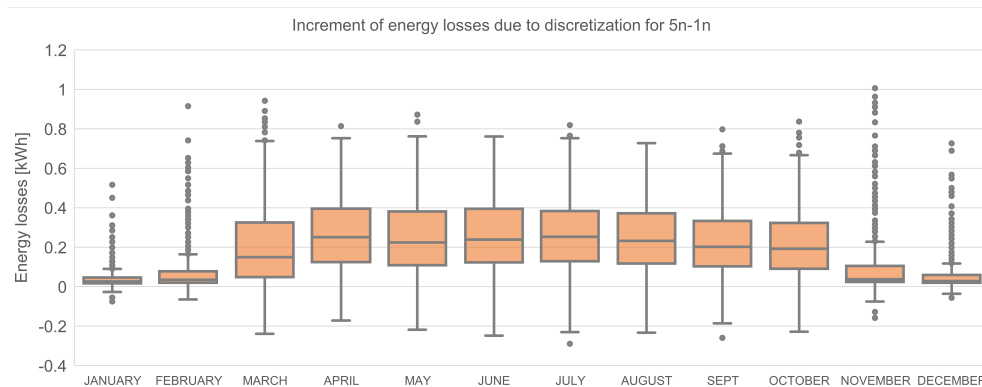


FIGURE 4.2: Increment of energy losses due to spatial discretization for 1n - 5n, ENaQ

Chart remarks:

- more than 75 % of the data are above 0 °C.
- Differences between models growth until 1 kWh.

- From November to February the differences are extremely low.
- From March to October the data distribution is bigger with a negative skew.
- In summer energy losses are so low that even some data points register negative values.

Regarding figure 4.1, the fact that differences are negative means the discretized model 5n underestimates the outlet temperature, especially in summer, where the distribution of the boxes is higher.

Boxes from March to October are asymmetric with a negative skew (wider data distribution at the bottom of the box) which means differences tend to decrease, and it is confirmed by the longer negative whiskers (bounded lines), and the concentration of all outliers (points) below each box, compared to the short whiskers and the absence of outliers at the top.

A 10 °C difference in outlet temperature between single and multi-node models have a significant impact on the efficiency of renewable energy systems such as photovoltaic (PV) solar panels, solar collectors and heat pumps. This is because the efficiency of these systems is closely tied to the temperature difference between the inlet and outlet of the pipe. Generally, the accuracy of the temperature sensors used i.e, in the solar collectors and the design of the system can affect the margin of error in the outlet temperature with a range from  $\pm 2$  °C to  $\pm 5$  °C, as explained by Sayigh et al, [33].

In terms of data distribution, the outlet temperatures differences differ widely from the energy losses, as can be seen in figure 4.1.

In figure 4.2, the fact that energy losses are positive means the spatial discretized method increases the sensibility to register the losses, especially from March to April where the distribution of the boxes is higher and the whiskers are longer. In contrast, the asymmetric box shape from November to February have a positive skew (the upper part of the box is bigger than the bottom), this means the data tend to be bigger than the median, also the small boxes size means the dispersion is smaller.

In other words, in those four months there are small differences between models, in comparison with the period from March to October, where the differences are wide higher with bigger boxes and longer whiskers. This behavior is a result of the influence of input parameters, mainly and directly correlated with the trend of the mass flow thorough the year as will be described in figure 4.6, but also partially affected by the soil and inlet temperature as presented in section 4.3.

The outliers are more present in the cold season because as the differences are very small, the dispersion is narrow and the whiskers are short, then values can easily trespass the boundary to become an outlier.

By comparing the two outlet parameters, energy losses and outlet temperature, the increment of energy losses has a range of 0,98 kWh which seems to be not significant, while the outlet temperatures decreases in an average of 6 °C, way more significant than the energy losses, hence, the discretization method has a stronger effect in the outlet temperature.

This becomes very relevant in the modelling of DH under LT conditions because the efficiency of the RE source, which is often in function of the temperature difference between the heat source and the outlet temperature, plays a critical role in maximizing the amount of energy that can be supplied to the network, then, an average deviation of 6 °C is crucial in terms of accuracy.

As the equation to calculate the energy losses 2.3d depends on the differences from the outlet temperatures, for now on the outlet temperature will be the main analyzed result.

Next, the results from scenario Lampoldshausen are presented in figure 4.3 that presents the deviations of outlet temperatures from the real data to the steady state (in blue) and to dynamic model (in orange) as follows:

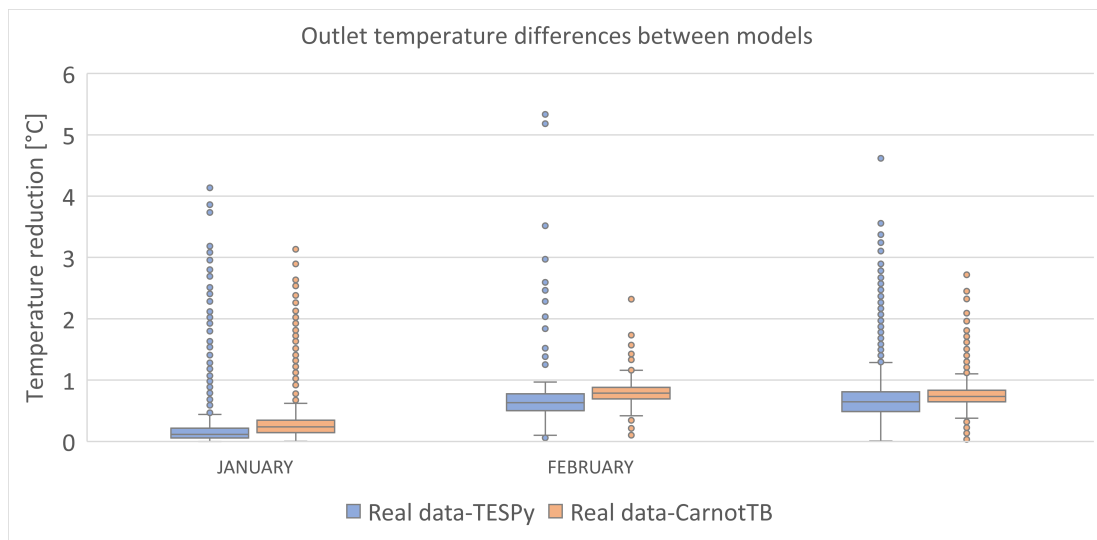


FIGURE 4.3: Reduction of the outlet temperature for 3 months between measurements data vs TESP<sub>y</sub> and measured data vs CarnotTB discretized, Lampoldshausen

Chart remarks:

- 100 % of data points are over 0 °C.
- Differences in January are bigger between real data and Carnot by 0,14 °C, while in March the differences are bigger between real data and TESPy by 0,14 °C
- The highest outlier in January is for Carnot 3,13 °C, while the highest in March is for TESPy with 4,6 °C
- In comparison with ENaQ, differences between single and multi node are much smaller.

First, the shape of the boxes indicate the distribution of the data is uniform, which means the differences are constant in terms of magnitude. The differences between single and multi-node simulations are not significant since the mass flow behavior, inlet temperature and heat transfer characteristics are similar throughout the network, while the soil temperature is linear.

The lack of a wider range of operation makes the system performance uniform, then a dynamic model cannot provide major differences than the steady state approach.

The trend of the differences can be detected mostly by the amount and direction of the outliers, and not from the data distribution due to the lack of prominent skews in boxes.

Comparing the differences between TESPy (steady state model) and CarnotTB (dynamic model) with the measurements (real data) can be seen in January both models are calculating approximately the same outlet temperature, but in February and March TESPy overestimate them. For example in March, the differences between models arise up including the outliers to 2,3 °C, the data distribution from TESPy is much bigger than CarnotTB. TESPy outliers are all positive meaning the trend is to only increase, in contrast with the outliers from CarnotTB that even when the skew is positive, it also has negative outliers meaning the trend is more stable.

At glance, differences between single and multi node models from ENaQ figure 4.1 are bigger than single and multi node differences from Lampoldshausen figure 4.3 orange boxes. This is clearly because both scenarios have different flow regimes and and temperature levels represented by their inlet parameters such as soil temperature, mass flow and inlet temperature, comparing them will lead to identify the effect of each one.



### 4.3 Influence of input parameters

The next part of this chapter analyzes the influence of each input parameter: Soil temperature, mass flow and inlet temperature, looking for evaluate the effect of the axial heat transfer. The two primary variables for the design and performance evaluation of a thermal network are outlet temperature and heat losses, and they are used as the basis of comparison for this analysis.

#### 4.3.1 Soil temperature

This input parameter is an assumption in both scenarios: In ENaQ, it was simulated with a sinusoidal wave that has a range of 11 °C. but for Lampoldshausen it was assumed as a linear constant of 12 °C as it is presented in table 4.3.

TABLE 4.3: Soil temperature range of operation for ENaQ and Lampoldshausen

Project	Maximum	minimum	Operation range.
ENaQ	13,79°C	2,2°C	11,5°C
Lampoldshausen	12°C	12°C	0°C

Subsequently, since Lampoldshausen has a linear constant, it does not affect the dynamic analysis. Therefore, only the behavior of the differences in heat losses and outlet temperature of ENaQ is illustrated in the figure 4.4.

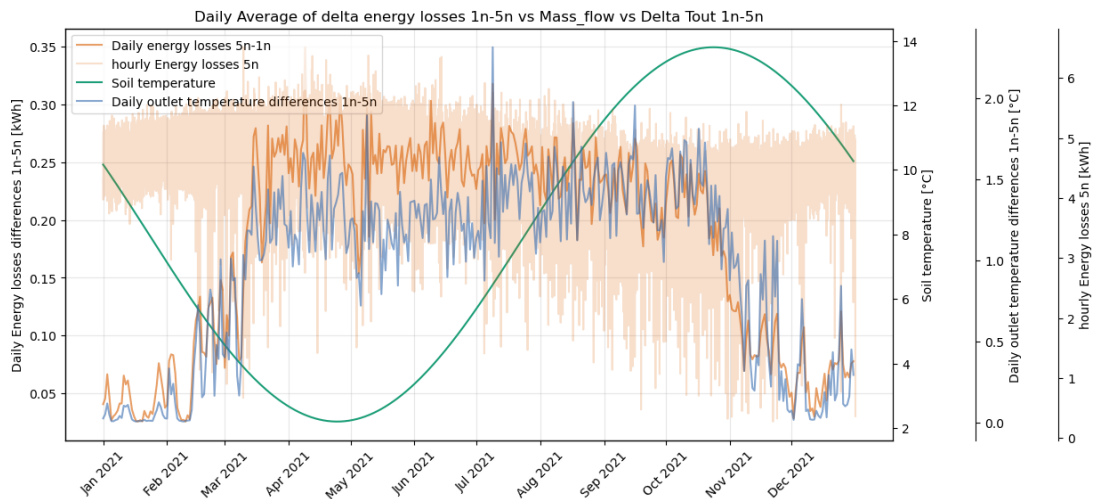


FIGURE 4.4: Delta energy values vs mass flow for 1n-5n, ENaQ, Carnot.

Chart remarks:

- Differences do not follow any trend guided by the soil temperature.
- Differences in heat losses and outlet temperature are presented with the absolute value to easily track them.
- In light orange is the trend of the hourly energy losses from simulation 5n. In dark orange is the daily trend of the energy losses differences between simulations 5n-1n.

Soil temperature has a strong influence in the energy losses as it was discussed in Maldonado's results [7], here is also perceived a slight sinusoidal behavior in clear orange flowing indirectly proportional the soil temperature in green. But the differences trend between models has not relation with the soil temperature shape.

Now, the influence of ENaQ scenario was simulated again but setting up the range of the soil temperature as a constant of 12 °C like in Lampoldshausen, the differences from both simulations are presented in the next figure:

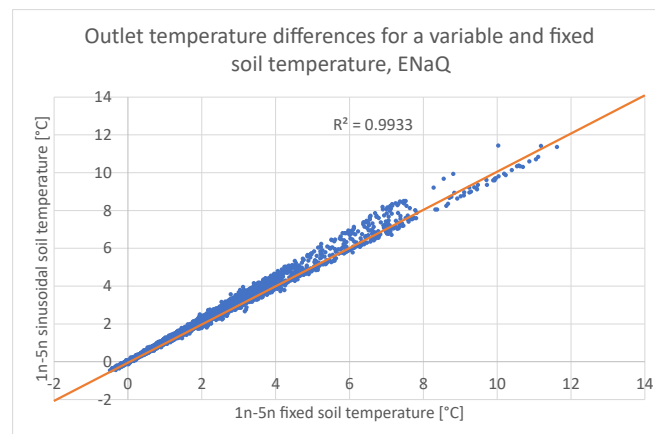


FIGURE 4.5: Reduction of the outlet temperatures for ENaQ with the sinusoidal soil temperature vs ENaQ with a fixed soil temperature of 12 °C

Chart remarks:

- The simulation with a constant soil temperature calculates in general smaller differences than the original simulation.
- The simulation with variable soil temperature registers a linear increment of differences from 0 °C until 9 °C, then it stops.

- On the other hand, the one with fixed soil temperature has a constant recording of differences within a small range, and it does not stop at 8 °C but keeps them somehow constant until reach 12 °C.

From this simulation can be conclude that soil temperature doesn't have a direct influence over the reductions in the outlet variables, but setting up the fixed soil temperature decreases the overall temperature distribution of the network, then the spatial discrete model cannot detect significant temperature gradients.

### 4.3.2 Mass flow

#### ENaQ

This parameter in scenario ENaQ has a range of 9.000 kg/h, and a range of 2.491 kg/h for Lampoldshausen, again the range in ENaQ is larger as presented in table 4.4.

ENaQ is analyzed first and later Lampoldshausen, at the end both of them are analyzed in parallel.

For ENaQ, two figures are presented, the first one 4.6 represents the energy losses and the behaviour of the differences in the outlet temperatures against mass flow.

In figure 4.7 two months were chosen to make a weekly profile and analyze the dynamic effect in more detail.

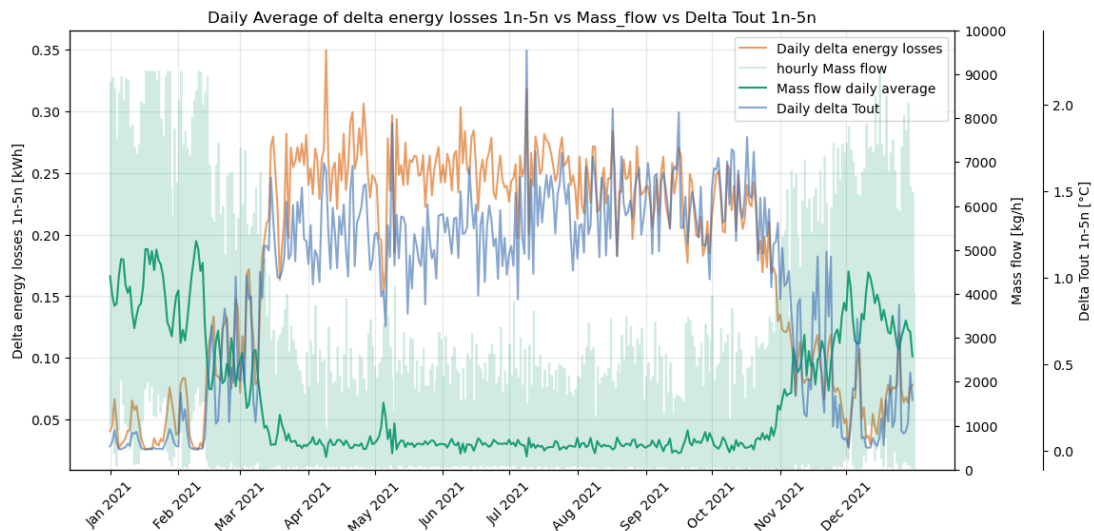


FIGURE 4.6: Energy losses and outlet temperature differences 1n-5n vs mass flow, ENaQ

Chart remarks:

- Delta values are indirectly proportional to mass flow.
- When mass flow is low outlet differences are high, on the other hand, high mass flows lead to small differences.

TABLE 4.4: Mass flow range of operation for ENaQ and Lampoldshausen

Project	Maximum	minimum	Operation range.
ENaQ	9.000 kg/h	0 kg/h	9.000 kg/h
Lampoldshausen	2.440 kg/h	4.931 kg/h	2.491 kg/h

Mass flow is presented with an hourly behavior in light green, and a dark green line for the daily behavior in order to make the comparison easier.

This is the parameter which influences the most when the spatial discretization takes place, as can be seen the differences in outlet temperature and energy losses in blue and orange respectively, both follow the same pattern than the mass flow in green, but with a mirror effect. Then, In figure 4.7 is presented a weekly profile for January due to its high mass flow and low differences in the first segment, and July due to its low mass flow and jagged differences in the second segment:

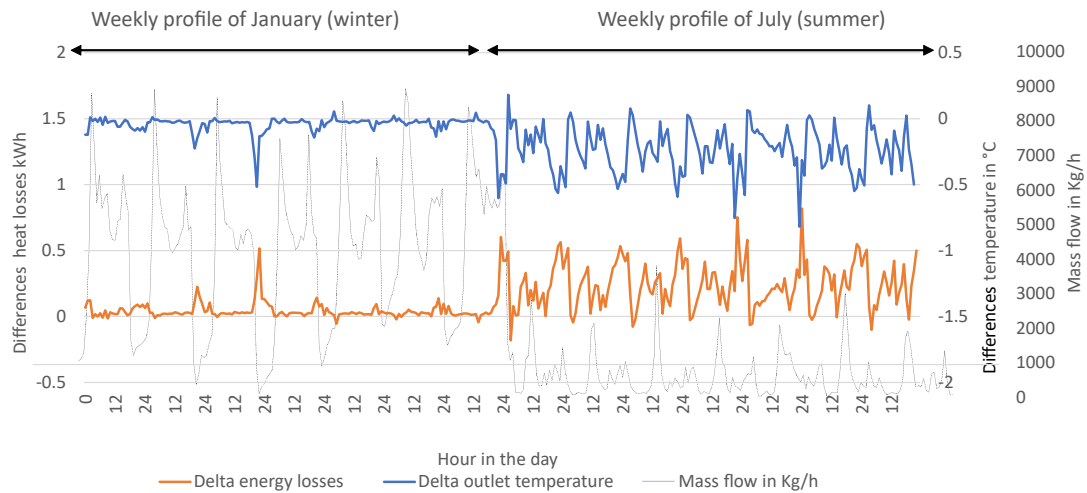


FIGURE 4.7: Weekly profiles for winter in January, and summer in July, in a dynamic analysis vs the mass flow, ENaQ

Chart remarks:

- On one hand, when mass flow is low differences are set in 0,5 °C approximately, mainly below 1.000 kg/h. On the other hand, high mass flows lead to small differences between models.
- In winter, represented by January on the left side, mass flow has a strong influence, mainly when it drastically drops under 1.000 kg/h, while in the same month high and quick increments even over 8.000 kg/h do not have the same effect.
- In summer, represented by July on the right side, mass flow is low due to the seasonal trend, constantly below 1.000 kg/h. This low mass flow do not change the magnitude of the differences but increases the frequency of the peaks, creating a jagged appearance.
- The only trend equally followed by the two compared months is the daily consumption behavior where the highest consumption is in the day, and the lowest in the night, as it is expected because the data comes from a urban neighborhood.

As stated before, the boundary of 1.000 kg/h denotes high importance, 60% of ENaQ database is below the boundary, then is necessary to analyze it in combination with the last input parameter, the inlet temperature.

After filtering the dataset below 1.000 kg/h, the inlet temperature is clustered in five equitable clusters of 2 °C each one, and to check the error of the spatial discreted models the differences from the reference moded with 5n, 10n and 20n models are also included. The error magnitude is measured with the RMSE. The correlation between the energy losses and outlet temperature for each discretized model can be found in appendix 6.3

Chart remarks from figure 4.8:

- High inlet temperatures trigger a higher RMSE in both analyzed variables.
- RMSE values for outlet temperature reductions are more equivalent between inlet temperature clusters, in contrast with the energy losses where there is a slight increment in the last 2 clusters.
- The bigger the number of nodes, the bigger the RMSE.

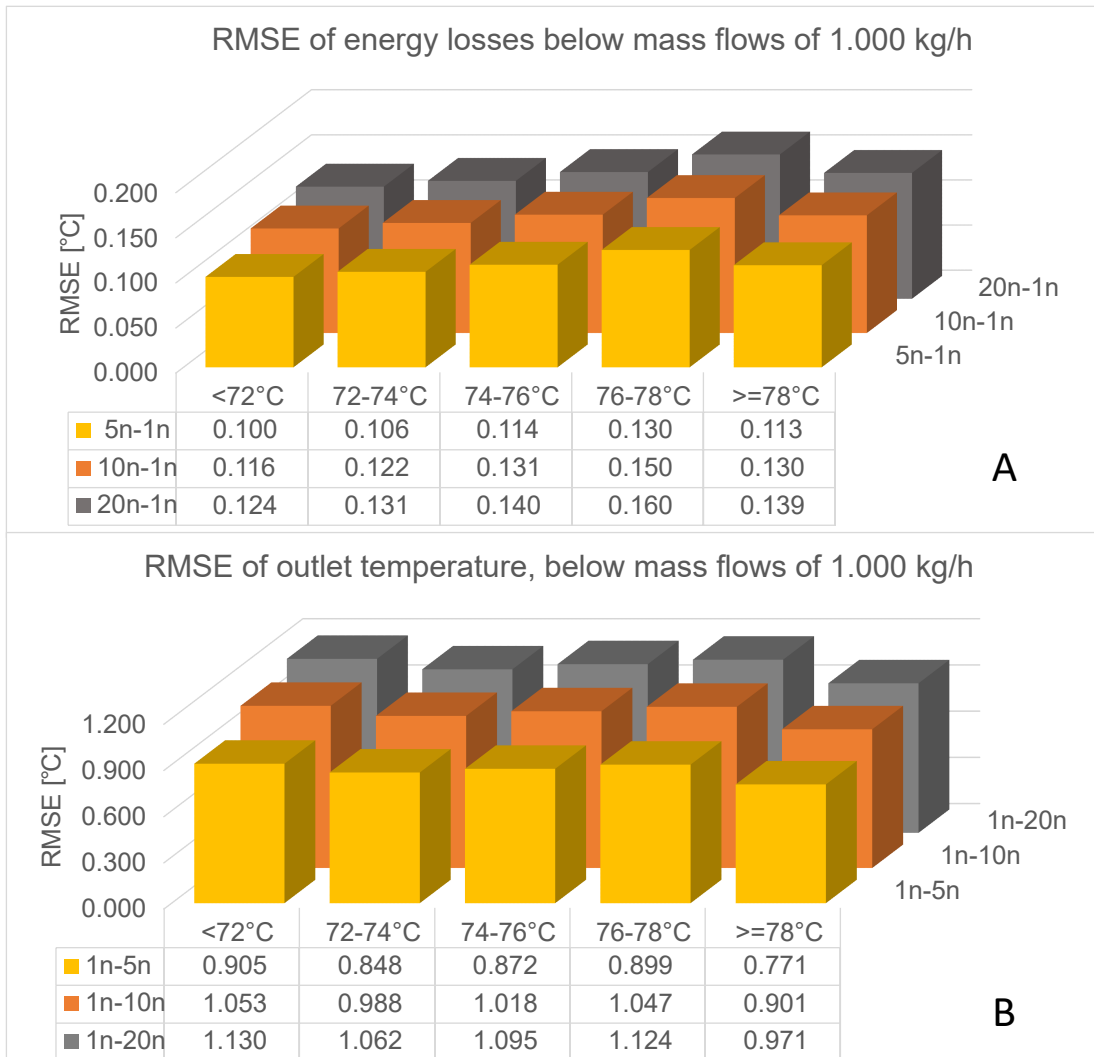


FIGURE 4.8: RMSE for heat losses and outlet temperature differences between single and multi nodes, for a clustered inlet temperature, ENaQ

It is important to recall from the methodology that generally the RMSE is measuring how close is the predicted data from the reference, the closer the magnitude to 0 the better, however as the reference model here is the simulation 1n, compared with 5n, 10n, and 20n, is reasonable that the model with less number of nodes, 5n, has the smaller RMSE.

But here the intention is to determine how much the space discrete model differs from the reference in function of the number of nodes, then a high RMSE value means the discrete model is capturing more differences than a steady state model.

From energy losses in figure 4.8 the main observation is the space discrete model records mayor increments at higher temperatures, the last cluster has the condition that even having the lowest concentration of data points because the network system is barely reaching its maximum temperature, that cluster still has bigger differences than the clusters below 74 °C.

From outlet temperature, chart B, the main observation is below 1.000 kg/h, the differences calculated by the models are constant with a similar RMSE magnitude, independently from the inlet temperature cluster, again the last cluster is an exception due to the same reason aforementioned.

The differences between simulations lies in the number of nodes, when the simulation split the pipe in more slides the dynamic model detects more changes over the time, but as can be seen the increment of the RMSE magnitude is not proportional to the number of nodes.

### Lampoldshausen

Next, the results of Lampoldshausen in relation with the mass flow are presented and discussed.

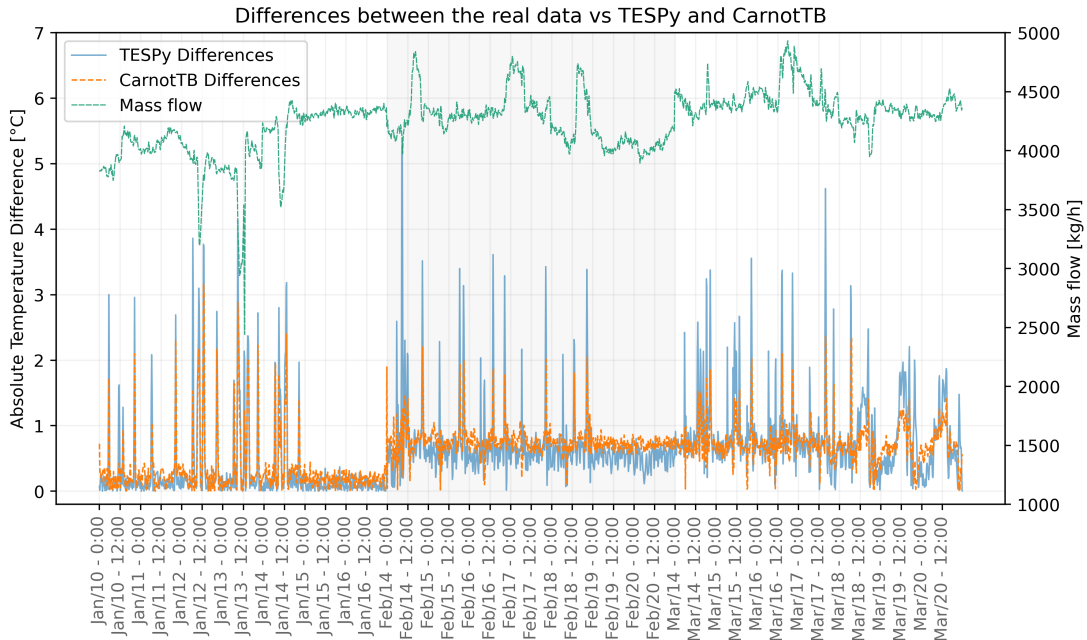


FIGURE 4.9: Reductions in the outlet temperature from the comparison between real data, TESPy and CarnotTB vs mass flow, Lampoldshausen

Chart remarks:

- In January, the most of the temperature differences between the two models appear to be consistent, with values mostly hovering around 0 °C. However, the magnitude of the peaks observed in this month is similar to those observed in the other two months.
- In February the temperature differences have a bit wider range than January, and while CarnotTB has a discreet fluctuation, TESPy fluctuation spreads from 0 °C to 3 °C, even 5 °C considering the single largest point in Feb/14 - 12:00.
- In March, the variation substantially increases in comparison with January, but still CarnotTB is more stable than TESPy, i.e, the trend from Feb/19 to Feb/20.
- Mass flow in green has not a visual direct influence.

The level of accuracy of both models is quite similar. In January, the differences in outlet temperature between real data and TESPy showed an average reduction of 0,33 °C, while the average reduction for CarnotTB was 0,35 °C. One month later, the average differences in outlet temperature slightly increased to 0,69 °C between real data and TESPy, and for CarnotTB, the average difference between real data and simulated data was 0,76 °C.

Finally in March, both models acquire greater variation, but here the magnitude of the underestimation of TESPy is higher than CarnotTB underestimation, with average temperatures of 0.85 °C and 0.73 °C respectively.

On the other hand, in this case, the differences between the models do not strictly align with the trend of the mass flow since the mass flow remains within a high range and does not reach low levels, such as the 1.000 kg/h observed in ENaQ. However, there are still perceptible changes in the outlet temperature trend as the mass flow decreases, particularly in January when the mass flow drops to its lowest level of 2.440 kg/h.

Additionally, in figure 4.9, TESPy, the blue jagged line may appear more erratic because it experiences more frequent fluctuations in values compared to orange line of CarnotTB. However, despite the visual differences, the overall average behavior of TESPy line is similar to CarnotTB line because the fluctuations eventually balance out and cancel the overflows each other.

As Lampoldshausen also has real data, is meaningful to visualize each model behavior separately, to do it figure 4.10 has the dynamic trend during the three available weeks,



the chart compare the steady state, dynamic model and the real data with the mass flow.

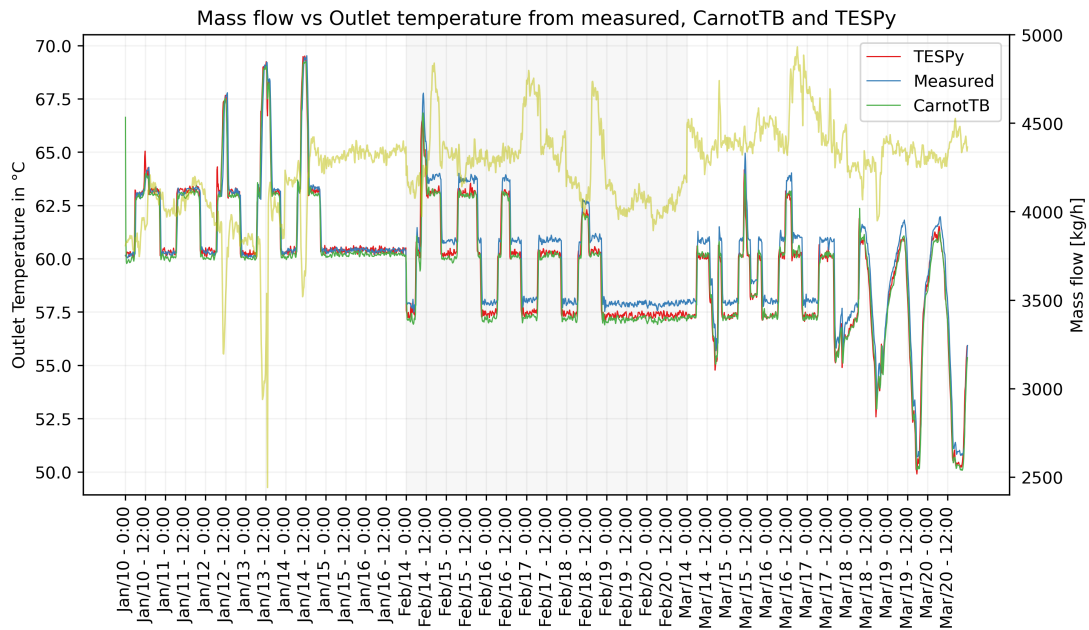


FIGURE 4.10: Outlet temperature from the the measured data, from the steady state model represented by TESPpy and from the dynamic model represented by CarnotTB, all compared with the mass flow, Lampoldshausen

Chart remarks:

- In February TESPpy and CarnotTB follow a very similar trend, but there is a noticeable gap between them and the measured data.
- March has a similar trend to February, but the small differences between steady state and dynamic model increase.

One of the biggest difference with EnaQ is that Lampoldshausen has a different demand pattern because is not a residential network, here the mass flow increases with the time.

In January, when the mass flow is low with elongated oscillation, both models closely follow the real data, however, TESPpy tend to overestimate and underestimate the outlet temperature when the mass flow drastically fluctuates. For example at Jan/10-11:45 am and Jan/12-7:00, with an overestimation of 1 °C and 2 °C respectively, and in Jan/13-13:00 with an underestimation of 2 °C, very high differences for a single point.

When the mass flow is almost constant, like for example, between January 15<sup>th</sup> and 16<sup>th</sup>, TESPy presents a better accuracy predicting the outlet temperature in contrast with CarnotTB, this means, in January the steady state approach is having a better accuracy than the dynamic approach. This fact is because as explained in the methodology, TESPy was designed to represent the network in these specific operating conditions in January, which adds more accuracy. Nevertheless, the mismatch between real data and both models is not really big, in overall, for the three weeks TESPy has an average outlet temperature underestimation of 0,33 °C, while CarnotTB outlet temperature underestimation is 0,62 °C. Then the total difference between them is 0,28 °C which is not a significant difference.

In February and March the mass flow is not going below 3.800 kg/h, and here a constant gap between models and measurements is observed. To analyze this matter, the figure 4.11 splits up the mass flow in three groups and presents the error.

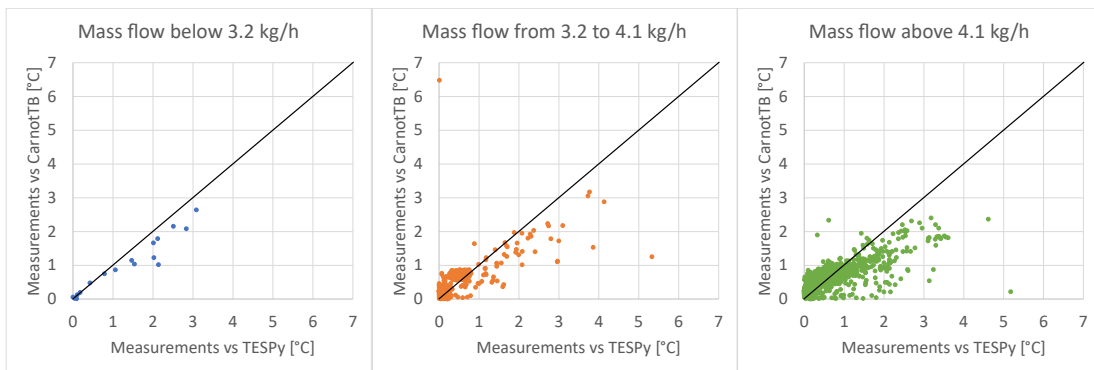


FIGURE 4.11: Correlation between steady state and dynamic models, clustered in 3 equitable ranges of mass flow, Lampoldshausen

Chart remarks:

- At low mass flows the predictability is almost perfect for CarnotTB, while TESPy has spread differences until 3 °C.
- Middle cluster shows an increment in TESPy's underestimation of the outlet temperature until 5 °C, while CarnotTB keeps the most of the differences below 1 °C.
- Up to 4.1 kg/h are more data points in the cluster, but the differences from real data do not significantly increase in temperature degrees.

This means the differences between models are better predicted by CarnotTB because their are not bigger than 1°C approximately, contrary to TESPy that always presents

wide data distribution and magnitude, it is important to state here the differences are calculated in absolute value, then in the final heat network simulations negative values can be compensated by positive values in order to normalize the prediction.

ENaQ differences are strongly influenced by mass flow but is not the same for Lampoldshausen, then, a new simulation is performed utilizing the original ENaQ data but changing the current mass flow for a sinusoidal wave which provides values between 2.440 kg/h and 4.931 kg/h, the same mass flow that Lampoldshausen has. The results of this simulation are presented in figure 4.12:

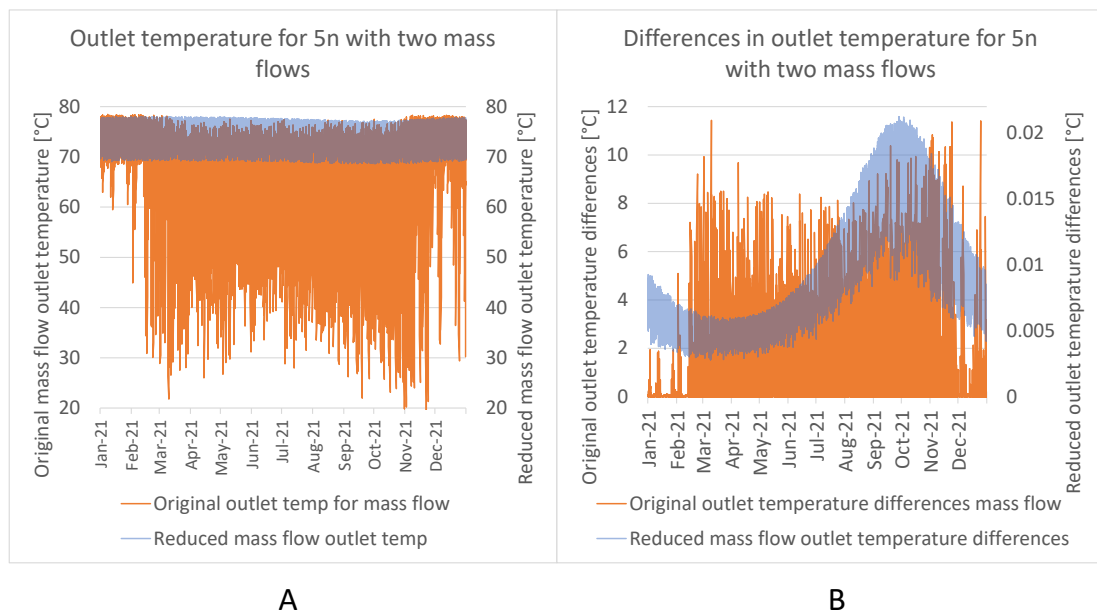


FIGURE 4.12: Outlet temperature behavior for two different mass flows A, differences in the outlet temperature for two different mass flows B.

Chart remarks:

- Outlet temperatures got a narrow variation determined by the range of inlet temperature with a very slight sine waveform inherited from soil temperature.
- Outlet temperature reductions have dramatically decreased not even reaching 0,5 °C.
- Outlet temperature differences are following the sinusoidal shape given by the new mass flow.

As the mass flow decreases, less heat is transferred to the fluid, which results in lower outlet temperatures. conversely, when the range of the mass flow is wide the

discretized model is capturing more details about the heat transfer process, leading to more accurate temperature predictions.

Lampoldshausen mass flow is medium-low size in comparison with ENaQ's mass flow, reducing its variation from 9.000 kg/h to 2.500 kg/h has still more influence over the differences in the outlet temperatures than the inlet or soil temperature current ranges.

From these results can be concluded the mass flow is the dominant factor in determining the outlet temperature differences when comparing space discrete and steady state model. As the mass flow decreases, the dynamic discrete models become more significant in terms of accuracy.

### 4.3.3 Inlet temperature

#### ENaQ

Inlet temperature is the last input parameter argued in this thesis. The heat supply for ENaQ has a very short range of variation of 8,9 °C as described in table 4.5. The inlet temperature trend during the year is presented in the same plot with the trend of the differences in energy losses and outlet temperature in figure 4.13.

TABLE 4.5: Inlet temperature range of operation for ENaQ and Lampoldshausen

Project	Maximum	minimum	Operation range.
ENaQ	78,9°C	70°C	8,9°C
Lampoldshausen	72,6°C	51,8°C	20,8°C

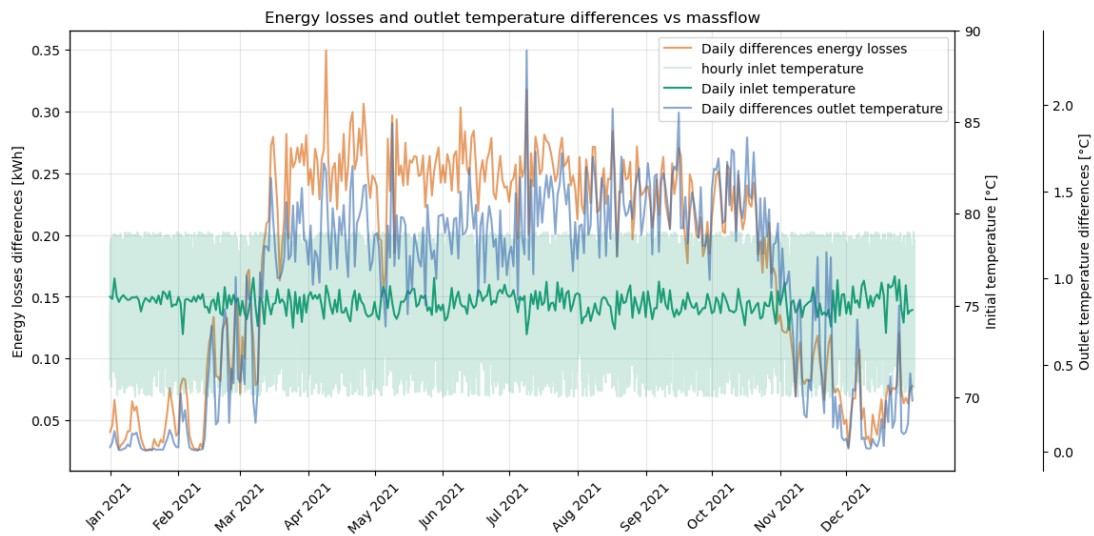


FIGURE 4.13: Differences in the energy losses and outlet temperature between 1n and 5n vs initial temperature, ENaQ

#### Chart remarks:

- Inlet temperature range is high and constant with small peaks that are not influencing the differences in the outlet variables.
- Inlet temperature has no seasonal or daily variation, and remains always over 70 °C as it is expected from a HT heating network.

There are no direct differences led by the inlet temperature under the predefined inlet parameters, and from the discrimination by clusters in the figure 4.8 is known that under 1.000 kg/h the inlet temperature with an operation range of 8,9 °C is not considerably affecting the differences between models.

#### Low Temperature synthetic profile.

One of the motivations to perform this master thesis is to investigate the conditions to integrate the RE, which is suitable under LT conditions.

As explained in the methodology, a LT network has inlet temperatures below 60 °C, then a synthetic inlet temperature profile was designed with inlet temperatures between 30 °C and 60 °C as presented in figure 3.7, and they are compared with the current ENaQ HT data with inlet temperatures between 70 °C to 80 °C utilizing the previously used RMSE method.

In this analysis, the simulations 5n, 10n and 20n are also considered to observe their differences against 1n. In the next figures energy losses in kWh and outlet temperature in °C are compared against the HT and LT profiles, but as they represent different physical quantities the units are described in the labels of the bars, then it is possible to compare only the magnitudes of the RMSE values to determine which one has a larger or smaller error, independently from their units.

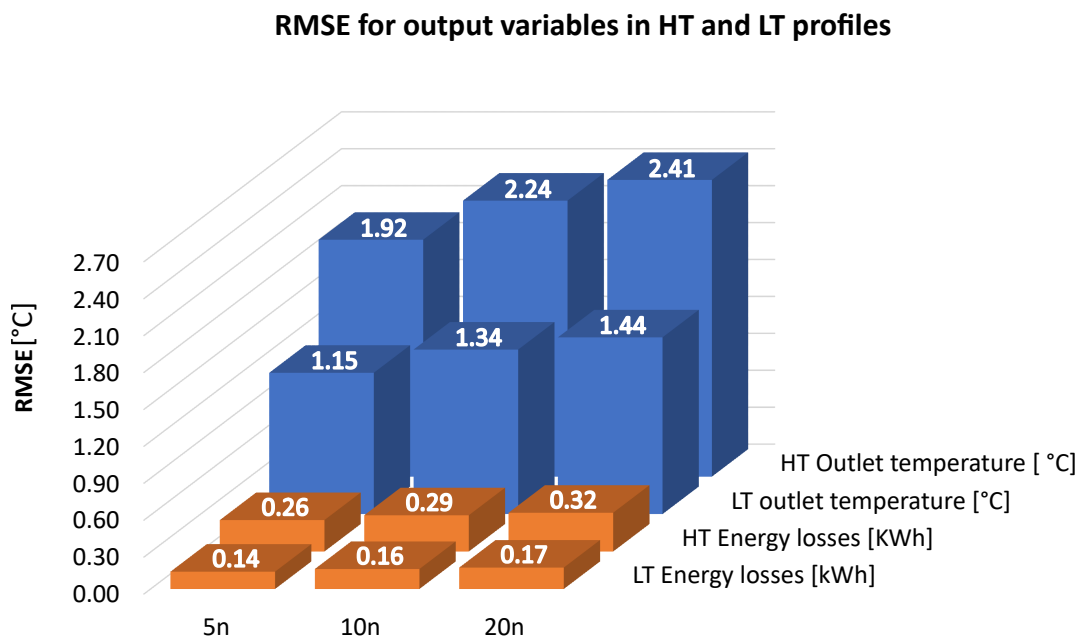


FIGURE 4.14: RMSE of the differences in output variables for HT and LT profile, ENaQ

Chart remarks:

- In orange, heat losses for both profiles have smaller RMSE than outlet temperatures.
- Compared with the HT, LT profile has the smallest RMSE.
- The increment in the RMSE is not proportional with the increment of number of nodes.

By comparing both temperature profiles, LT presents the minor magnitude for the two output variables, which means the inlet temperature actually could influence the differences in two different ways:

On one hand, HT conditions supply more heat to the network increasing the network temperature which is beneficial for the spatial discrete model because can capture more temperature gradients, and LT conditions reduce the thermal operation range of the system making it relatively uniform, then the discretization loses its effect.

On the other hand, this LT profile has, in fact a lower temperature, but also a short range of operation of 30 °C, that even being bigger than HT range of 10 °C, due to the low temperature it is not enough to create a meaningful temperature difference, then the overall system temperature range is smaller and can be fulfilled with linear predictions such as the steady state model.

### Lampoldshausen

Inlet temperature in Lampoldshausen starts at 51,8 °C until 72,6 °C, it has 19 °C more of operation range, but 6 °C colder, in figure 4.15 is the relationship with the outlet temperature reductions.

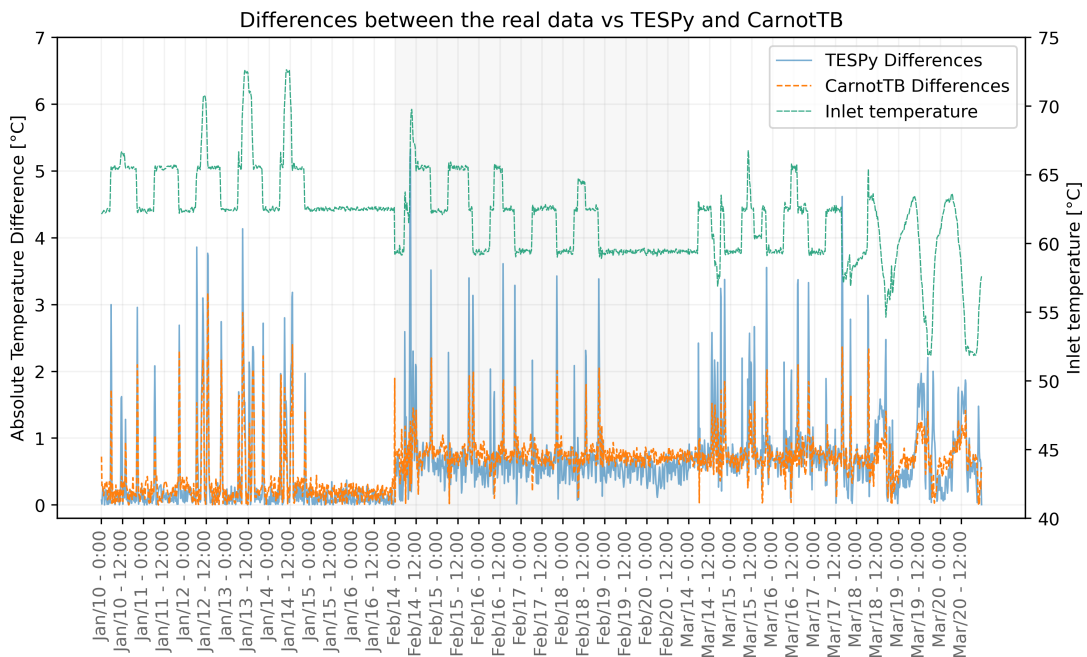


FIGURE 4.15: Reductions in the outlet temperature from the comparison between real data, TESPpy and CarnotTB vs inlet temperature, Lampoldshausen

#### Chart remarks:

- Inlet temperature has a strong correlation with the reductions of the outlet temperature between real data and models.

- When the inlet temperature is constant, there are not significant peaks in the reductions.
- Steep increments and falls from inlet temperature are directly related with the peaks in the differences between real data and models.

For Lampoldshausen, in comparison with ENaQ, the inlet temperature is the dominant input parameter which defines the reductions trend of the outlet temperature.

For Lampoldshausen, the inlet temperature not only affects the differences between models, but also affects the outlet temperatures, as can be observed in the following figure 4.18:

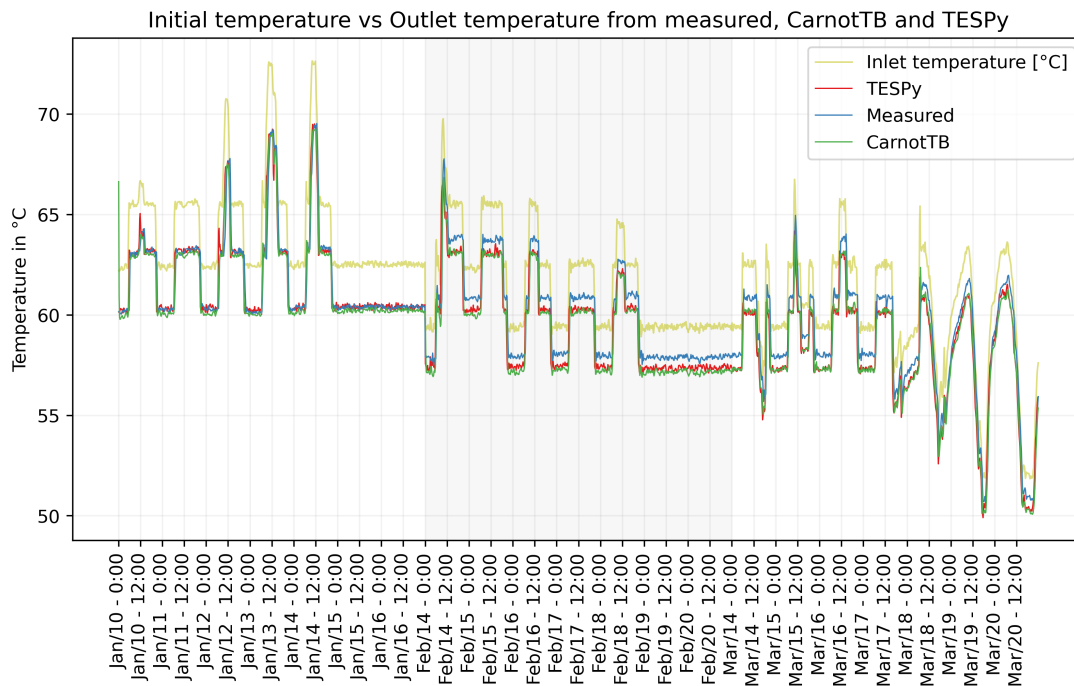


FIGURE 4.16: Outlet temperature from the real data, TESPpy and CarnotTB vs inlet temperature, Lampoldshausen

Chart remarks:

- Inlet temperature trend is closely followed by models and real data.
- Gap between models decreases when inlet temperature decreases.

To examine the changes in inlet temperatures and the differences between the real data and models, figure 4.17 provides a close-up view of a two-day period from February



14<sup>th</sup> to February 16<sup>th</sup>. This time the differences are not displayed in absolute values, but with the real orientation either negative or positive.

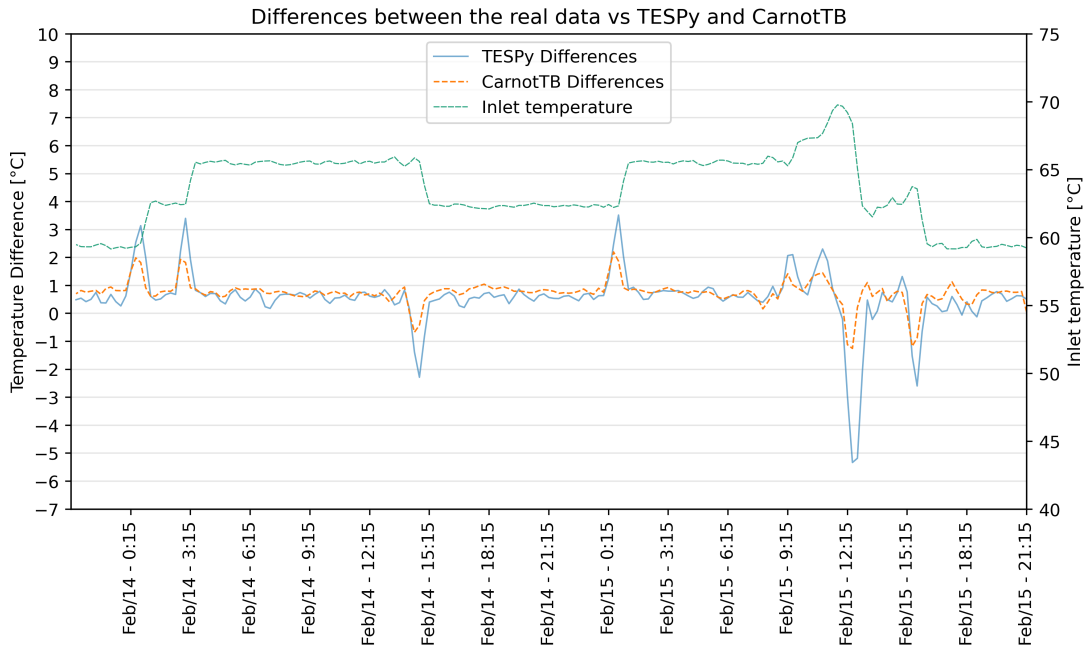


FIGURE 4.17: Outlet temperature from the real data, TESPy and CarnotTB vs inlet temperature, Lampoldshasen

- When inlet temperature is uniform the differences between models are not trespassing 1 °C, but when the temperature changes, either up or down, the models react and predict a change with the same direction.
- The trend of the differences corresponds to the magnitude of the changes in inlet temperature.

From this result can be stated that the trend of outlet temperature and its differences between models do not mandatory follow the input parameter mass flow, but also inlet temperature and soil temperature, then, this depends on the size and magnitude of each one to become in the predominant variable.

Next, the inlet temperature is split in three clusters to analyze the behavior of each model in ranges of 7 °C.

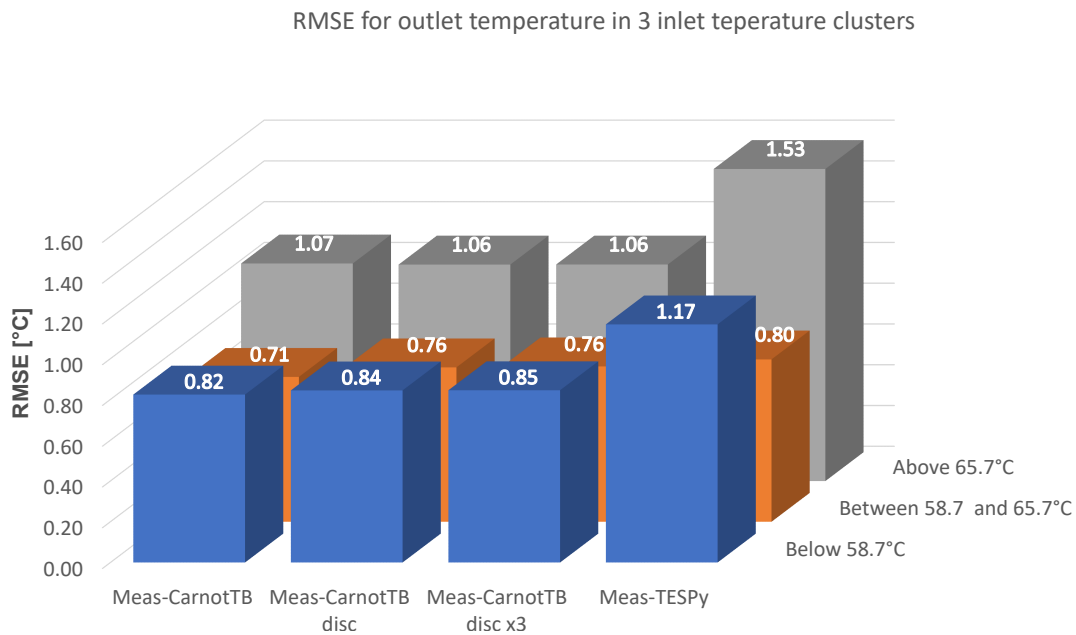


FIGURE 4.18: Clustered inlet temperature to get the RMSE of the differences in outlet temperatures, Lampoldshasen

Chart remarks:

- The differences between single node model and measurements (Meas-CarnotTB) has a better RMSE than the models with more nodes (CarnotTB disc and CarnotTB disc x3), however, the differences between them are too small, then increasing the number of nodes has not a significant effect in this system.
- TESPpy has the worst RMSE overall, but in the cluster between 58,7 °C and 65,7 °C the difference from CarnotTB is 0,04 °C, which can be neglected.
- Above 65 °C is the cluster with highest RMSE, but the variation between models in CarnotTB is negligible.
- CarnotTB and TESPpy have a similar accuracy, and CarnotTB has not real improvement when spatial discrete models take place, contrary to it, below 65,7 °C, the RMSE magnitude increase for them, which means the predictions are less accurate.

For lampoldshausen the RMSE method has the real meaning about how far are the simulations from the real data because real data is available, that is the big difference with ENaQ, and can be compared with figure 4.14.

In addition to Figure 4.18, the figure 4.19 illustrates the absolute differences in outlet temperature for each spatial discrete model.

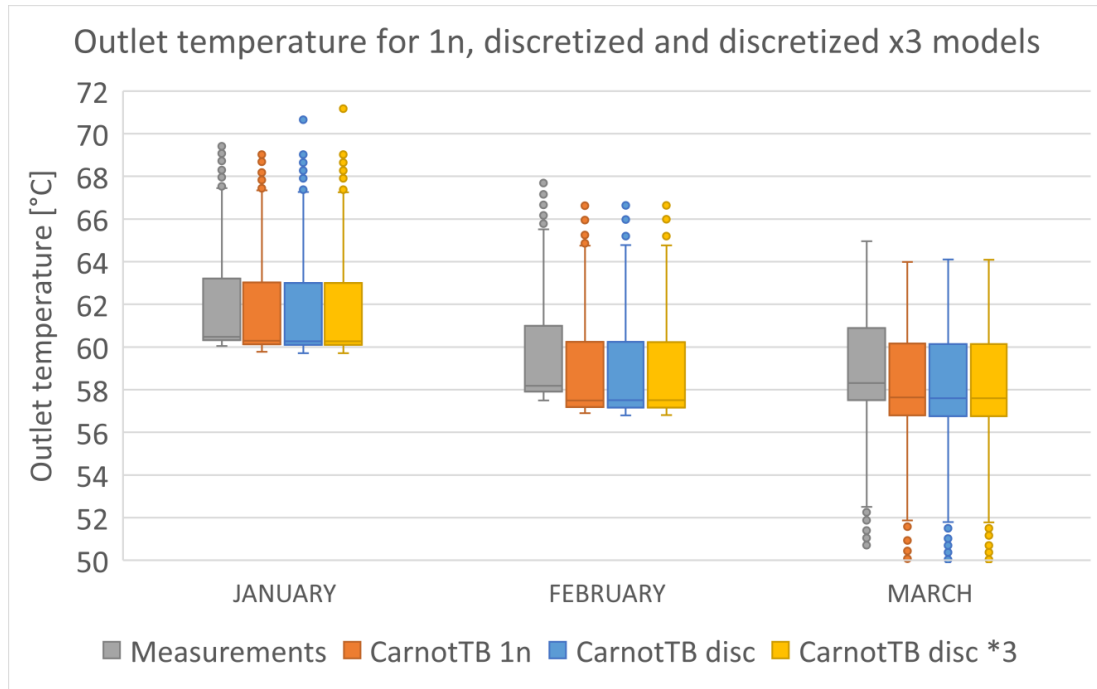


FIGURE 4.19: Box and whiskers chart for outlet temperatures for the different spatially discretized models, Lampoldshausen

The reason why the outlet temperature differences are correlated with the inlet temperature in this scenario might be attributed to the high mass flow levels and the limited range of operation, which results in a minor impact.

Additionally, the temperature distribution in the real DHN is relatively uniform. Then, the inlet temperature is the dominant factor in determining the outlet temperature, and the spatially discrete models are not adding much value to the simulations.

Finally, in figure 4.19 shows that there is a minimal change in the outlet temperatures for each discretized model, despite the increase in the number of nodes. The only noticeable difference is between the real data and the simulations, as all the simulations have the same data distribution, start and end of whiskers, and outliers.

Hence, the impact of axial heat transfer on predicting the outlet temperature is insignificant.

### Increment of nodes in TESP<sub>y</sub>

The last simulation is analyzing the effect of discretize the pipe but in the TESP<sub>y</sub> model designed by Maldonado [7], a model that has not been compared with the models from this thesis as described in the last part of the methodology.

ENaQ energy losses for one year are shown against the mass flow in a logarithmic scale in the figure 4.20. First chart are the total energy losses, the green cloud of dots represents the losses from the original model single node, purple and pink cloud of points represents the 3n and 10n simulations, second chart is the correlation between 1n-3n and 1n-10n, the differences between multi node models and the original single node model.

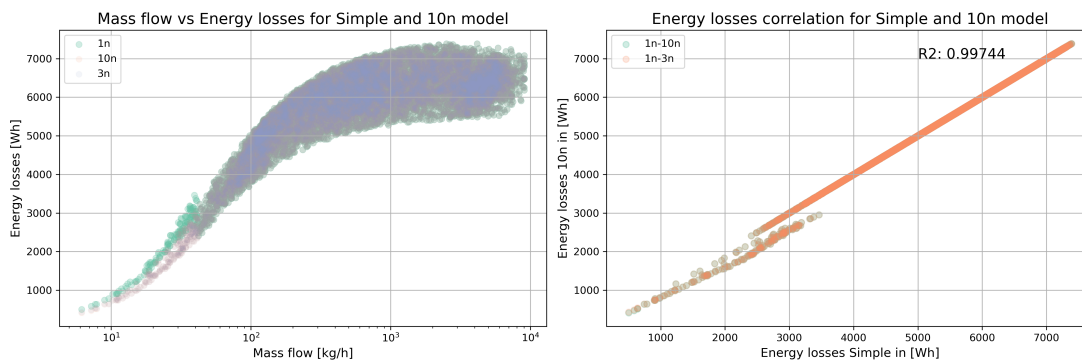


FIGURE 4.20: Energy losses from 1n-3n and 1n-10n comparison, ENaQ, TESP<sub>y</sub>

#### Chart remarks:

- Energy losses have a strong linear relationship between both simulations.
- Below mass flows of 100 kg/h and energy losses of 3.000 Wh, TESP<sub>y</sub> has a mismatch between models.
- In general the losses are the same for all the models, but the models 3n and 10n have a better behavior when calculating the losses at low mass flows.

At glance, there is not a strong effect caused by the discretization, neither by the number of nodes, but below 3.000 Wh losses and mass flows below 100 kg/h, can be perceived a small change in the trend, where the spatial discrete models shows a smoother trend better aligned with the rest of the points, in contrast with the jump of the green cloud of points in the same conditions. This jump in model 1n is because the software solver is unstable and tend to increase the losses at extremely low mass

flows, but as soon as the network reach a minimum mass flow of 40 kg/h the software recovers its stability and provide smaller energy losses.

This behavior indicates the discretization can be used to get more accurate energy losses at very low mass flows, prediction of losses can be reduced until 3.000 Wh in the initialization of the simulation, as demonstrated in the second chart of figure 4.20.

Regarding the outlet temperatures, the figure 4.21 presents in the overall outlet temperatures for 1n and 10n, as well as the correlation from simulation 1n versus 3n and 10n, and again the dicretized model has better trend when the mass flow is low.

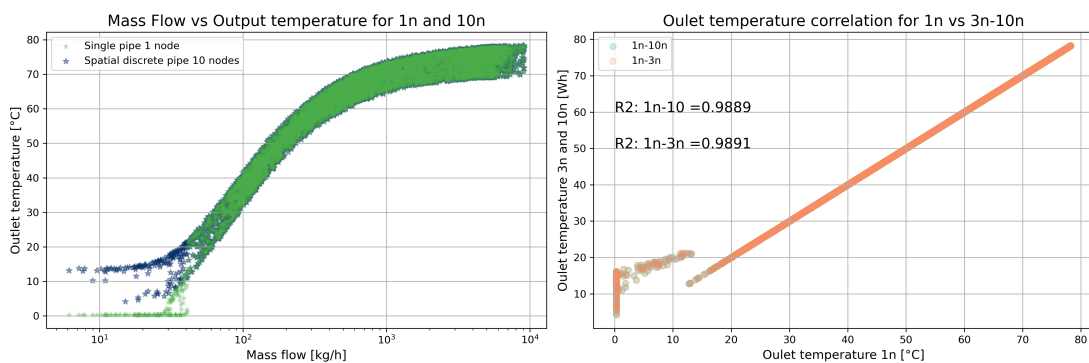


FIGURE 4.21: Initialization behaviour for outlet temperatures for 1n vs 3n and 10n, ENaQ, TESPpy

Chart remarks:

- Outlet temperature have a strong linear relationship between both simulations, with a R-squared up to 0,98.
- Below mass flows of 100 kg/h and outlet temperatures of 22 °C , TESPpy generates a mismatch between models.
- In general the losses are the same for all the models, but spatial discrete models 3n and 10n have a better behavior when recording the outlet temperatures at low mass flows.

First chart has in green the outlet temperatures from the single node model 1n, and in dark blue the losses from model 10n. Similar to energy losses the spatial discrete models present a better trend at low mass flows, the last outlet temperature not reached by the software is 22 °C, after that TESPpy algorithm gets stable and both models 1n and 10n start to calculate the same outlet temperatures.

In comparison with Maldonado's results, when the discretization is included the system is able to calculate outlet temperatures even with the smallest mass flow value from the provided database 6.14 kg/h. At 6.14 kg/h simulation 1n was registering temperatures of 0,28°C, while simulation 3n reached 9,6 °C and simulation 10n reached 13,12 °C. But in the overall calculated losses the magnitude of differences can be neglected due to its size in comparison with the scale of the whole network.

Additional considerations must be taking into account, i.e. in figure 4.20 the energy losses from 1n displayed as 0 Wh, must be understood as "not recorded value" instead of TESPy calculated 0 wh of energy losses, this is due to the results from calculation of the losses are under TESPy boundaries, mainly numerical boundaries in the algorithm, then losses cannot be recorded and default values are provided, in this case 0 Wh.

Regarding outlet temperatures the boundary for single node model 1n was detected that on 22 °C is where the software gains stability, and from that threshold the software calculates the same outlet temperature as the 10n model. Below this threshold the minimum recorded value is 0,28 °C, but again, it doesn't mean TESPy calculated that specific temperature, 0,28 °C is the default value provided when the solver cannot calculate it.

Those specific values such as a minimum amount of mass flow of 40 kg/h running through the pipe and minimum outlet temperature of 22 °C that are defining when the system jumps from unstable to stable are unique for ENaQ conditions, should not be generalized because those are defined by size of temperature gradients in the network.

Digging on the reasons directly on TESPy algorithm calculations, was found the solver crashes when the differences in the partial derivatives are less than  $1 \times 10^{-4}$  [17]. Then when outlet temperature reaches the same value of the soil temperature and the difference between them is less than that, the algorithm assumes 0°C has been reached. In this specific case, ENaQ 1n, crashes when the outlet temperature and soil temperature are in 10 °C.

Then, the difference between single and multi node seems to be due the effect of spatial discretization, but as the only task was to split the pipe, not axial heat transfer was included which disproves the theory. The reason is due to by discretizing the pipe the jumps between thermal gradients gets smaller so then the algorithm can keep a track of them until it reaches the last node giving a real calculated values and not default numbers.

## Chapter 5

# Conclusions and future work

### 5.1 Conclusions

Following the same order from the sections before, general conclusions will be stated to connect with each finding, and later a summary of results with recommendations and ideas for future work.

On one hand, dynamic models have shown a significant impact on the accurate prediction of thermal behavior in comparison with the steady state models. Dynamic models provide a more accurate representation of the the thermal performance of the heat networks by effectively predicting the effect of change the operating conditions and system setups, such as variations in input parameters like input temperatures and mass flow.

On the other hand, when including the axial heat transfer, which is the principal parameter when discretizing a pipe in a dynamic model, have shown important differences when the network has enough thermal gradients inducing changes in the results of the different models, but when the system temperature distribution tend to be uniform, discretizing the pipe does not significantly affect the results.

The effect of thermal inertia in a network spatially discretized model is to increase the energy losses and decrease the outlet temperatures. Depending on the parameters distribution, the energy losses can vary around 1 kW/h, while the outlet temperature can achieve differences of between 5 °C and 10 °C.

As it was presented, ENaQ outlet temperature differences are led by the mass flow because from the three input parameters, mass flow has the wider range of operation with 9.000 kg/h, while the soil temperature has a range of operation of 11°C, and the inlet temperature has a range only of 9°C.

Additionally, this scenario have the biggest differences between models due to the mass flow because, apart from the greater range of operation, it achieves low mass flows below 1.000 kg/h the most of the time, and low mass flows rise bigger and relevant differences between models.

To have a better perspective about how wide must be the operation range of the mass flow in order to keep being the natural leader of differences between steady state and dynamic models, the original mass flow from ENaQ was changed to have a higher level and shorter operation range, from 2.440 kg/h to 4.930 kg/h, which means the variation was reduced to have only 2.440 kg/h. The result is the differences are still following the mass flow trend, but as consequence less differences in the outlet temperature and energy losses are detected.

Finally, from the synthetic profile analysis, the main observation is the differences between models when the inlet temperature is under low temperature conditions, is that the accuracy of the models improve. In terms of outlet temperature, the RMSE changed from HT to LW 1,92 °C to 1,15 °C respectively.

These results encourage investigating in more detail the LT networks and also low mass flow regimes.

In the case of Lampoldshausen, differences are lead by the inlet temperature because from the three input paramaters, inlet temperature has the wider range of operation of 20 °C, the mass flow has a range of operation of 2.440 kg/h and the soil temperature has not range of operation because it is constantly in 12 °C, it doesn't vary. In this specific scenario, 20 °C of inlet temperature dominates over a mass flow with an operation range of 2.440 kg/h.

Then, can be concluded the dominant parameters are the ones having the bigger range of operation in each scenario, because it provides more range to detect thermal gradients and widened the thermal distribution in the system.

Regarding the soil temperature, in the context of DN where the pipes are mainly buried, this parameter is not leading due to its temperature change is smooth, short and uniform, however, it still provides a minimum thermal range that contributes with the discretized model to capture more temperature gradients, then it indirectly influences the output variables differences.

From here can be conclude a dynamic model is worthed when the system distribution is wide enough to calculate significant thermal gradients, however it is not clear how to categorize if a system is uniform or not.



Regarding the accuracy of steady state systems against dynamic systems, this master thesis has shown when the network and its transient behavior are changing significantly over time, is better to select a dynamic model for analysis. Like scenario ENaQ where there are several levels of mass flow and temperatures within hours, then when the spatial discrete model is applied it can capture more details and for example decrease the outlet temperature until 10 °C.

Additionally, the effect of discretize the pipe is more consistent when the number of nodes are increased because the accuracy improves, however the improvement is not bigger than 1 °C in the model with the most of the nodes, then the level of accuracy can be relative depending on the boundaries defined by the researcher.

In contrast is the Lampoldshausen scenario, due to the short thermal ranges given by the inlet parameters, the system can be analyzed with the steady state model and still obtain sufficient accurate results.

When Lampoldshausen was analyzed with the dynamic and spatial discrete approaches it was seen there is not a significant improvement, oppositely, due to network is relatively uniform the dynamic results can even go worse because it is forced to get temperature gradients in low temperature distributions creating extra overestimation and underestimation of the losses, additionally, a spatially discretized model introduces additional thermal resistance at the nodes, which can reduce accuracy.

For the specific projects here analyzed within the predefined boundaries, it was enough to split the pipe in slices that represent approximately 20% of the original length, by doing this the smaller slices were 2m and 5m, considering the average length for both projects is 120m. This decision was taken considering there are only three main input and two output parameters to analyze, and the scope of the present thesis is to compare the differences within a range where they are significant, but for DHN with a wider average pipe length and meant to analyze more and/or different parameters, additional considerations should be taken in order to use a trade-off between accuracy and computational cost to select the optimal number of nodes.

Finally, from the discretization in TESP<sub>y</sub> can be concluded the number of nodes do not strongly affect the results, just by splitting the pipe in 2 or 3 nodes is enough to face that small variation in the initialization of the simulation even when it is very small. Additionally this method could be used if the researcher needs to analyze a steady state system with very low mass flows, because it was seen that is how the solver can work with them, but then the additional computational effort gets too high

in comparison with the magnitude of the results from single node model. It is true that that can be compensated by installing libraries which handle simplest values, but as explained in section 4.1 is recommended using a trade-off between accuracy and computational cost [23] and this method is inaccurate as well as inefficient, then is suggested not to follow it.

## 5.2 Future work

During the time performing this thesis some phenomena were observed which worth to be further investigated because, even when they are related to this master thesis topic, they are out of scope. In total there 3 main ideas and are presented here as possible future work.

When investigating the influence of the mass flow and inlet temperature, an important effect has been seen in the comparison of steady state and dynamic models, specially when the mass flow is low and under LT conditions, together they predict much better the thermal gradients and is suggested to deeply investigate on them.

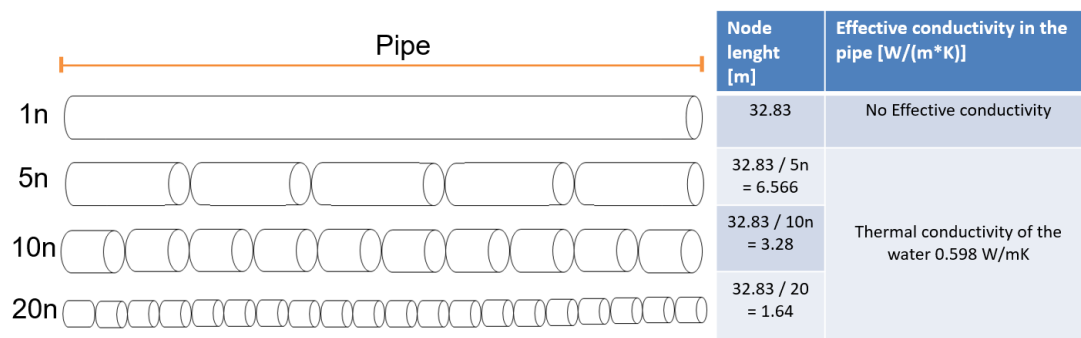
When analyzing the impact of each input parameter it was noticeable that the range of operation really matters, in this master thesis the systems are defined as uniform and not uniform, but must be investigated the quantitative boundaries to categorize when a system can be considered "uniform" enough to be analyzed only with a steady state approach, and when the system has enough thermal gradients to be analyzed with a dynamic approach.

The method here utilized to determine the optimal number of nodes was done using simple mathematical methods and a constrained sensitivity analysis, however there are too many other factors and parameters that were not taking into account and is suggested investigate on them to have have a better guide to define the optimal number of nodes for a spatial discrete model.

## Chapter 6

# Appendix

### 1 Scenario



Model	Dynamic	
Project name	Carnot Toolbox / Simulink	
ENaQ	1 tube n=1	2
	1 tube n=Nodes	

#### HYPOTESIS:

Carnot toolbox, Matlab  
Heat transfer coefficient ✓  
Pipe's thermal inerthia ✓

Observe the influence of the axial heat transfer, energy losses and outlet temperature differences will be achieved.

FIGURE 6.1: Description of the scenario 1, discretization visualization and hypothesis

## 2 Scenario

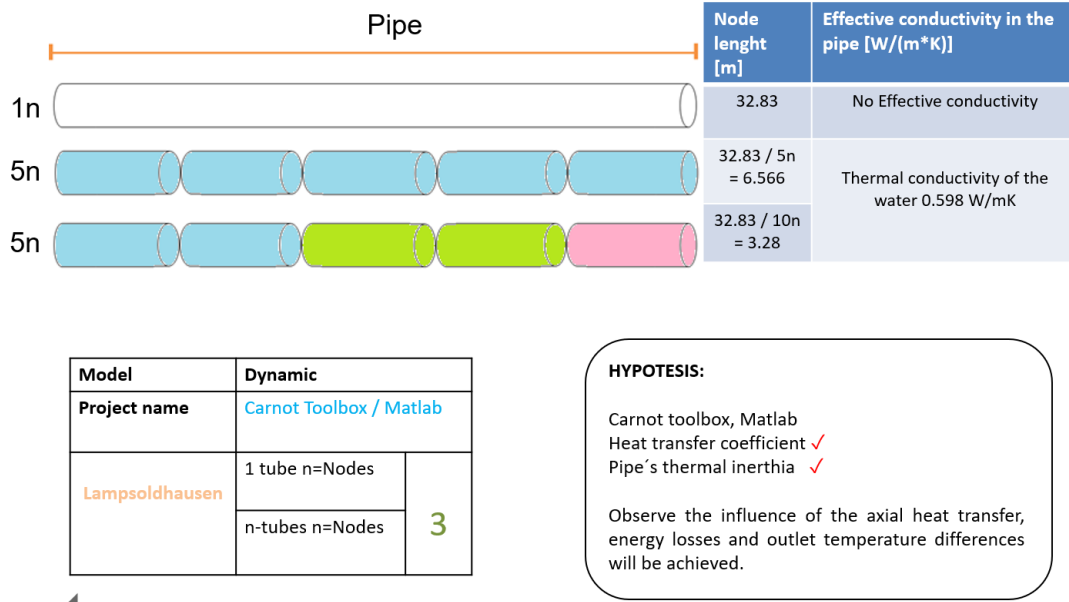


FIGURE 6.2: Description of the scenario 2, discretization visualization and hypothesis

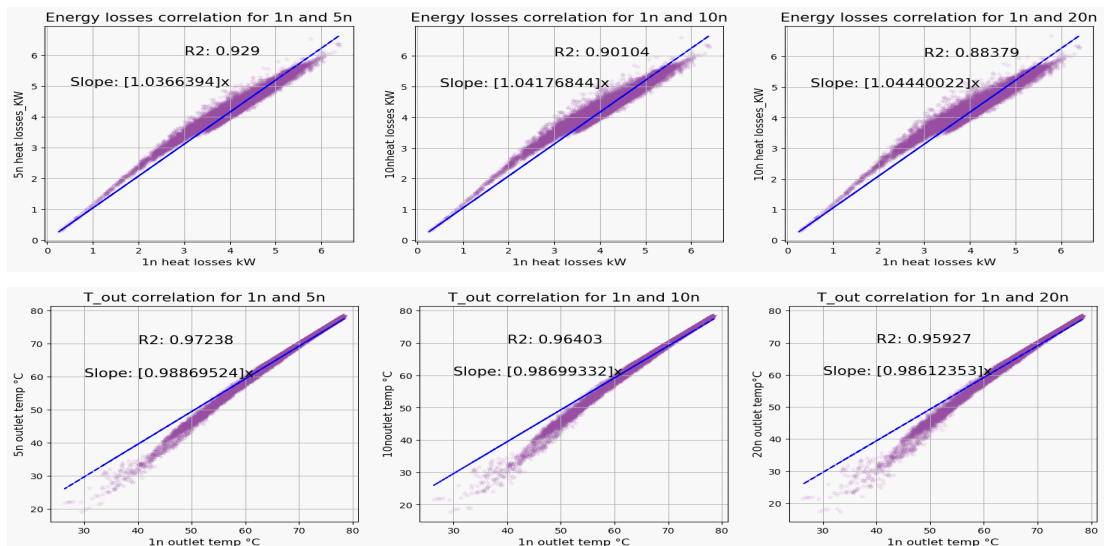


FIGURE 6.3: Correlation for energy losses and losses temperature for scenario 1, between 1n and discreted models 5n, 10n 20n

# Bibliography

- [1] *What is net zero?* <https://netzeroclimate.org/what-is-net-zero/>, Accessed on 2023-04-10.
- [2] J. Chontanawat, "Relationship between energy consumption, co2 emission and economic growth in ASEAN: Cointegration and causality model," *Energy Reports*, vol. 6, no. Supplement 1, pp. 660–665, 2020, ISSN: 2352-4847. DOI: <https://doi.org/10.1016/j.egyr.2019.09.046>. [Online]. Available: <https://www.sciencedirect.com/science/article/pii/S2352484719305517>.
- [3] I. E. Agency, *District heating and cooling*, <https://www.iea.org/reports/district-heating>, Accessed on April 11, 2023, 2020.
- [4] Agora Energiewende, *Heat transition 2030: Pathways for heat supply in germany*, [https://www.agora-energiewende.de/fileadmin/Projekte/2016/Sektoruebergreifende\\_EW/Heat-Transition-2030\\_Summary-WEB.pdf](https://www.agora-energiewende.de/fileadmin/Projekte/2016/Sektoruebergreifende_EW/Heat-Transition-2030_Summary-WEB.pdf), Accessed on: 2023-04-12, 2016.
- [5] A. Pina, S. Mansouri, N. Martins, and P. Ferrão, *Thermal energy storage systems for building applications: A state-of-the-art review*, 2018. DOI: 10.3389/fenrg.2018.00103. [Online]. Available: <https://www.frontiersin.org/articles/10.3389/fenrg.2018.00103/full>.
- [6] M Despeisse, M Baumers, P Brown, *et al.*, *Future cities: A glimpse through the lens of urban metabolism*, 2016. DOI: 10.3389/fbuil.2016.00022. [Online]. Available: <https://www.frontiersin.org/articles/10.3389/fbuil.2016.00022/full>.
- [7] D. T. Maldonado Castro, "Simplified modelling approach for district heating networks, potential and application for high and low temperature regimes," Ph.D. dissertation.
- [8] P. Duran, H. Torio, P. Schönfeldt, *et al.*, "Technology pathways and economic analysis for transforming high temperature to low temperature district heating systems," *Energies*, MDPI Energies, vol. 14, no. 11, 2021. [Online]. Available: <https://elib.dlr.de/142999/>.
- [9] B. van der Heijde, M. Fuchs, C. Ribas Tugores, *et al.*, "Dynamic equation-based thermo-hydraulic pipe model for district heating and cooling systems," *Energy*

- Conversion and Management*, vol. 151, pp. 158–169, 2017, ISSN: 0196-8904. DOI: <https://doi.org/10.1016/j.enconman.2017.08.072>. [Online]. Available: <https://www.sciencedirect.com/science/article/pii/S0196890417307975>.
- [10] J. Maurer, O. M. Ratzel, A. J. Malan, and S. Hohmann, “Comparison of discrete dynamic pipeline models for operational optimization of district heating networks,” *Energy Reports*, vol. 7, no. 4, pp. 244–253, 2021, ISSN: 2352-4847. DOI: 10.1016/j.egypr.2021.08.150. [Online]. Available: <https://www.sciencedirect.com/science/article/pii/S235248472100754X>.
- [11] H. Lund, S. Werner, R. Wiltshire, and S. Svendsen, “4th generation district heating (4gdh): Integrating smart thermal grids into future sustainable energy systems,” *Energy*, vol. 68, pp. 1–11, 2014, ISSN: 0360-5442. DOI: <https://doi.org/10.1016/j.energy.2014.02.089>. [Online]. Available: <https://www.sciencedirect.com/science/article/pii/S0360544214002369>.
- [12] D. Schmidt, A. Kallert, M. Blesl, *et al.*, “Low temperature district heating for future energy systems,” *Energy Procedia*, vol. 116, pp. 26–38, 2017, ISSN: 1876-6102. DOI: 10.1016/j.egypro.2017.05.052. [Online]. Available: <https://www.sciencedirect.com/science/article/pii/S1876610217322592>.
- [13] A. Wrzalik, “Smart district heating networks in the era of energy transformation,” *System Safety: Human - Technical Facility - Environment*, vol. 4, no. 1, pp. 58–66, 2022. DOI: 10.2478/czoto-2022-0007.
- [14] V. Verda and E. Guelpa, “Modelling approach for fast simulation and optimization of large district heating networks,” *TECNICA ITALIANA-Italian Journal of Engineering Science*, vol. 63, no. 2-4, pp. 397–403, 2019.
- [15] E. Guelpa, A. Sciacovelli, and V. Verda, “Thermo-fluid dynamic model of large district heating networks for the analysis of primary energy savings,” *Energy*, vol. 184, pp. 34–44, 2019, ISSN: 03605442. DOI: 10.1016/j.energy.2017.07.177.
- [16] S. R. Jones, M. Gillott, R. Boukhanouf, *et al.*, “A system design for distributed energy generation in low-temperature district heating (ltdh) networks,” *Future Cities and Environment*, vol. 5, no. 1, p. 2, 2019. DOI: 10.5334/fce.44.
- [17] F. Witte, *Thermal engineering systems in python, documentation*. [Online]. Available: <https://tespy.readthedocs.io/en/main/index.html>.
- [18] F. A. U. of Applied Sciences, *Carnot blockset user’s guide: Version 1.0*. [Online]. Available: <https://docplayer.net/11219095-Carnot-blockset-version-1-0.html>.
- [19] A Dénarié, M Aprile, and M Motta, “Heat transmission over long pipes: New model for fast and accurate district heating simulations,” *Energy*, vol. 166, pp. 267–276, 2019, ISSN: 0360-5442. DOI: 10.1016/j.energy.2018.09.186.

- [Online]. Available:  
<https://www.sciencedirect.com/science/article/pii/S0360544218319583>.
- [20] F. Witte and I. Tuschy., *Tespy: Thermal engineering systems in python*.
- [21] J. Maurer, O. M. Ratzel, A. J. Malan, and S. Hohmann, "Comparison of discrete dynamic pipeline models for operational optimization of district heating networks," *Energy Reports*, vol. 7, no. 4, Supplement, pp. 244–253, 2021, ISSN: 2352-4847. DOI: <https://doi.org/10.1016/j.egyr.2021.08.150>. [Online]. Available:  
<https://www.sciencedirect.com/science/article/pii/S235248472100754X>.
- [22] S. V. Patankar, *Numerical Heat Transfer and Fluid Flow*, 1st. Hemisphere Publishing Corporation, 1980, ISBN: 9780891165223.
- [23] N. Haddou, N. Ait-Messaoudene, K. Guedri, and M. S. Guellil, "Optimal number of nodes for simulation of the transient behavior of a plate heat exchanger using the finite volume method," *Journal of Thermal Analysis and Calorimetry*, vol. 133, no. 1, pp. 117–126, 2018. DOI: 10.1007/s10973-018-7089-y.
- [24] ENaQ Project, *Energetisches nachbarschaftsquartier fliegerhorst oldenburg (enaq)*. [Online]. Available:  
<https://helleheide.de/energetisches-nachbarschaftsquartier-fliegerhorst-oldenburg-hauptseite-projektvorstellung/>.
- [25] ENaQ Project, *Das smart city living lab oldenburg*. [Online]. Available: <https://www.enaq-fliegerhorst.de/teilprojekte/>.
- [26] C. von Ossietzky University of Oldenburg, *Enaq (energetic neighbourhood oldenburg air base)*. [Online]. Available: <https://uol.de/enaq>.
- [27] DLR, *Green light for energetic neighbourhood in oldenburg*. [Online]. Available: [https://www.dlr.de/content/de/artikel/news/2017/20171208\\_gruenes-licht-fuer-energetisches-nachbarschaftsquartier-in-oldenburg\\_25384.html](https://www.dlr.de/content/de/artikel/news/2017/20171208_gruenes-licht-fuer-energetisches-nachbarschaftsquartier-in-oldenburg_25384.html).
- [28] *Dlr lampoldshausen: Test center for rocket engines and space propulsion systems*.
- [29] *Dlr lampoldshausen in openstreetmap webpage*.
- [30] S. Weisberg, *Applied Linear Regression*. John Wiley Sons, 2005, ch. 1.
- [31] S. A. McLeod, *What does a box plot tell you?* <https://www.simplypsychology.org/boxplots.html>, 2019.
- [32] V Vignesh, D Pavithra, K Dinakaran, and C. Thirumalai, *Data analysis using box and whisker plot for stationary shop analysis*, Tirunelveli: IEEE, 2017. DOI: 10.1109/ICOEI.2017.8300874.

- [33] A. Sayigh and S. A. Kalogirou, *Comprehensive Renewable Energy, Volume 3: Solar Thermal Systems: Components and Applications*, ch. 13. Solar Collectors.